 doi:10.20944/preprints202009.0141.v1

Nonlinear approximations to critical and relaxation processes

Simon Gluzman
Materialica + Research Group, Bathurst St. 3000, Apt. 606, Ontario M6B 3B4, Toronto, Canada (simongluzmannew@gmail.com)

Abstract

We discuss methods for calculation of critical indices and amplitudes from the perturbative expansions. They are demonstrated for the Stokes flow through 2D and 3D channels enclosed by two wavy walls. Efficient formulas for the permeability are derived in the form of series for small values of amplitude. Various power-laws are found in the regime of large amplitudes, based only on expansions at small amplitudes. Lubrication approximation is shown to break down, but accurate formulas for the effective permeability for arbitrary values of the wave amplitude are derived from the expansions. The technique developed for critical phenomena is applied then for relaxation phenomena. The concept of time-translation invariance is discussed, its spontaneous violation and restoration considered. Emerging probabilistic patterns correspond to a local breakdown of time-translation invariance. Their evolution leads to the time-translation symmetry complete (or partial) restoration. We estimate typical time extent, amplitude and direction for such restorative process. The new technique is based on explicit introduction of origin in time. After some transformations we come to the exponential and generalized, exponential-type solution with explicit finite time scale, which was only implicit in initial parametrization with polynomial approximation. The concept of crash as a relaxation phenomenon, consisting of time-translation invariance breaking and restoration, is put forward. COVID-19 related mini-crash in the time series for Shanghai Composite is discussed as an illustration.

 doi:10.20944/preprints202009.0141.v1

1 Introduction

We are interested in the behavior of a real function $\Phi(x)$ of a real variable $x \in [0, \infty)$. Let this function be defined by a complicated problem that does not allow for an explicit derivation of the function form. But what can be done is only the use of some kind of perturbation theory yielding asymptotic expansions about $x_0 = 0$,

$$\Phi(x) \sim \sum_{n=0}^{\infty} c_n x^n. \tag{1}$$

Note that exact solutions are exceptionally rare and even then mostly represented as series. Out task is to obtain an accurate approximate solution represented as series, and recast them into convergent expressions by means of analytically expressed approximants.

The simplest way to make sense of such perturbative results or extrapolate is to apply the Padé approximants $P_{n,m}(x)$ [1]. However, solutions to many problems, e.g., nonlinear equations exhibit irrational functional behavior, which cannot be well described by Padé approximants or sometimes these are not applicable at all. Approximate solutions in the class of irrational functions can be constructed by invoking such irrational functional forms as self-similar root approximants. In principle, it could be possible to employ the additive self-similar approximants as such. But it would be a pity to forget the well developed techniques of Padé approximants. So, the question has been advanced whether it would be possible to modify the use of Padé approximants in such a way that to extend their applicability to the class of irrational functions. The desired modification can be performed by splitting the sought solution into two factors, one, represented by iterated root approximants or factor approximants, taking care of the irrational part of the solution, and the other being a Padé approximant, characterizing the rational part of the solution. The so corrected Padé approximants are applicable to a larger class of problems and are well defined even for those cases, where the standard Padé approximants cannot be used [2]. Many more applications of the Padé approximants and their modifications could be found in [3].

Extrapolation methods attempt to, from the knowledge of several terms of an asymptotic expansion (1), as $x \to 0$, to find the limit corresponding to $x \to \infty$. The variable $x > 0$ can represent, e.g., a coupling constant

 doi:10.20944/preprints202009.0141.v1

or concentration properly transformed. Interpolation problem consists in constructing such a representation for the sought function $\Phi(x)$ that would reproduce the small-variable, as well as large-variable expansions, providing an accurate approximation for the whole domain $[0, \infty]$.

The Padé approximants $P_{M,N}$ are nothing else but ratio of the two polynomials $P_M(x)$ and $Q_N(x)$ of the order M and N, respectively. If $M = N$ the approximant is called a diagonal Padé approximant of order N. Usually, $Q_N(0) = 1$. The coefficients of the polynomials are derived directly from the coefficients of the given power series [1] from the requirement of asymptotic equivalence to the given series or function $\Phi(x)$. When there is a need to stress the last point, we simply write $PadeApproximant\,[\Phi[x], n, m]$, adopting a reduced notation from $Mathematica^{®}$.

The Padé approximants locally are the best rational approximations of power series. Their poles determine singular points of the approximated functions [1]. But the functions in the vicinity of their critical points, in general, are non-rational. Therefore the direct use of Padé approximants for functions exhibiting critical behavior is impossible. A Padé approximant can have a pole that could be associated with a finite critical point, but the related critical index would be an integer, while usually critical indices are not integers. The same concerns the large-variable behavior where the power of x is always an integer. The holomorphy of diagonal Padé approximants in a given domain implies their uniform convergence inside this domain [4].

When the character of the large-variable limit is known, one can invoke the two-point Padé approximants. Two-point Padé are applied when in addition to the expansion about $x_0 = 0$, given by (1), an additional information is available and contained in the expansion about $x = \infty$.

There are four main technical approaches to constructing approximants with the goal to optimize their performance. The first approach is conventional, also called accuracy-through order, and is based on progressive improvement of quality with adding new information with the approximants becoming more and more complex. It is exemplified in construction of Pad'e and Euler super-exponential approximants, factor, root and additive approximants [2].

Second approach leads to corrected approximants. The idea is to ensure the correct form of the solution already in the starting approximation with some initial parameters. The initial parameters should be corrected by asymptotically matching with the truncated series/regressions in increasing

 doi:10.20944/preprints202009.0141.v1

orders. So, instead of increasing the order of approximation as prescribed by the first approach, one can correct the parameters of the initial approximation [2, 9]. So, the form of the solution is not getting more complex, but the parameters take more and more complex form with increasing order. Corrected approximants will complement the third approach, when there are no solutions within the framework of the third approach.

In the third approach predominantly adopted in Section 4, we keep the form and order of approximants the same in all orders, but let the series/regressions evolve into higher orders. Independent on the order of regression, we construct the same approximant, based only on the first order terms, only with parameters changing with increasing order of regression. In the framework of effective first order theories, we employ exponential approximants.

In the fourth approach the critical index by itself is considered as control parameter, sometimes even as a control function, to be determined from optimization procedure described in the Section 2.2, following [50]. Some other optimization techniques based on introduction of an additional control parameters, were proposed in [51, 52].

2 Critical index and relaxation time

A real function $\Phi(x)$ of a real variable x is said to exhibit critical behavior, with a critical index α, at a finite critical point x_c, when in the vicinity of this point it behaves as

$$\Phi(x) \simeq A(x_c - x)^{\alpha}, \text{ as } x \to x_c - 0 \, . \tag{2}$$

The function can tend to infinity, if the critical index α is negative, or to zero, if this index is positive. When the value of critical index is known in advance, the problem consists in finding the critical amplitude A. In [2], various ways to calculate A were discussed.

The critical behavior can also occur at infinity, where the function behaves as

$$\Phi(x) \simeq Ax^{\alpha}, \text{ as } x \to \infty \, , \tag{3}$$

with the critical index α. Respectively, the function can tend to infinity, if α is positive and to zero, if α is negative. The critical behavior at infinity can formally be interpreted as the case, where the critical point is located at infinity.

 doi:10.20944/preprints202009.0141.v1

Critical phenomena are widespread [50], ranging from the field theory to hydrodynamics. And it is an important problem of defining the related critical indices. However, for realistic physical systems the sole thing one can do is to resort to perturbation theory for obtaining the behavior of the sought function at small variable,

$$\Phi(x) \simeq \Phi_k(x), \text{ as } x \to 0 \, , \tag{4}$$

where the function is approximated by an expansion

$$\Phi_k(x) = 1 + \sum_{n=1}^{k} c_n x^n \, . \tag{5}$$

Such expansions are usually asymptotic and strongly divergent not allowing for their use at finite values of the variable.

The critical exponents can be found by using standard definition of the critical index. The techniques employed here express critical index directly, as the limit of explicitly calculable approximants. Critical index can be estimated from a standard representation called here a "single pole" approximation for the following derivative (or else called a *DLog* transformation for the series $\Phi(x)$),

$$\mathcal{B}_a(x) = \partial_x \log(\Phi(x)) \simeq \frac{-\alpha}{x_c - x}, \tag{6}$$

as $x \to x_c$, thus defining critical index as the residue in the corresponding single pole. The pole here defines the critical point x_c, while the critical index is given by the residue

$$\alpha = \lim_{x \to x_c} (x - x_c) \mathcal{B}_a(x).$$

To the *DLog*-transformed series one would consider applying the Padé approximation. As is known [1], for a given expansion of order k, one can construct the whole table of Padé approximants. This means that defining the critical indices through the *DLog* Padé method is not a uniquely defined procedure. And different Padé approximants can result in basically different values. Then it is not clear which of these quantities to prefer. Usually, outside of the immediate vicinity of the critical point a diagonal Padé approximant is typically assumed for the residue estimation.

Preprints (www.preprints.org) | NOT PEER-REVIEWED | Posted: 6 September 2020 doi:10.20944/preprints202009.0141.v1

When a function, at asymptotically large variable, behaves as in (3), then the critical exponent can be defined similarly, by means of the $DLog$ transformation. It is represented by the limit

$$\alpha = \lim_{x\to\infty} x\mathcal{B}_a(x) \ . \tag{7}$$

Assume that the small-variable expansion for the function $B_a(x)$ is given. In order that the critical index be finite it is necessary to take the asymptotically equivalent approximants behaving as x^{-1} as $x \to \infty$. It leaves us no choice but to select the non-diagonal Padé $P_{n,n+1}(x)$ approximants, so that the corresponding approximation α_n is finite. One can also apply, in place of Padé, some different approximants. To this end one should apply the transformation,

$$z = \frac{x}{x_c - x} \ \Leftrightarrow \ x = \frac{zx_c}{z+1} \tag{8}$$

to the original series and reduce the problem of finding critical index to the previous case.

To simplify and standardize calculations different, and more powerful approximants, called self-similar factor approximants have been introduced in Refs. [6]. The k-th order self-similar factor approximant reads as

$$\mathcal{F}_k^*(x) = c_0 \prod_{i=1}^{N_k} (1 + \mathcal{P}_i x)^{m_i} \ , \tag{9}$$

where

$$N_k = \tfrac{k}{2}, \quad k = 2, 4, \ldots; \quad N_k = \tfrac{k+1}{2}, \quad k = 3, 5, \ldots \tag{10}$$

and the parameters $\mathcal{P}_i$ and m_i are defined typically from the standard procedure, solely from various constraints on the sought function. For example, by expanding expression (9) in powers of x, comparing the latter expansion with the given power series for small x, and equating the like terms in these expansions. When the approximation order $k = 2p$ is even, the above procedure uniquely defines all $2p$ parameters. When the approximation order $k = 2p+1$ is odd, one sets some additional condition dictated by the problem specifics, and uniquely defining all other parameters. Their singularities are associated with critical points and phase transitions [6]. The singularity can be also located at ∞. For long series it is typical that their accuracy improves with inclusion of larger and larger number of terms from available expansions. But it is not clear how even attempt to improve factor approximants

 doi:10.20944/preprints202009.0141.v1

when the series are short, unless some additional asymptotic(or point-wise) information on the critical point is available.

2.1 Relaxation time

When a function, at asymptotically large variable, decays as

$$\Phi(t) \simeq A \exp(\frac{t}{\tau}) \qquad (t \to \infty) \; , \tag{11}$$

with negative τ. Then the relaxation time is $-\tau$, and can be found as the limit

$$\frac{1}{\tau} = \lim_{t\to\infty} \frac{d}{dt} \ln \Phi(t) \; . \tag{12}$$

Assuming that the small-variable expansion for the function is given by the sum $\Phi_k(t)$, the corresponding small-variable expression for the effective relaxation time can be found,

$$\frac{1}{\tau_k(t)} = \frac{d}{dt} \ln \Phi_k(t) \; , \tag{13}$$

which can be expanded in powers of x, leading to

$$\tau_k(t) = \sum_{n=0}^{k} b_n t^n \; , \tag{14}$$

with the coefficients b_n expressed through c_n of the original series (1). Applying to the obtained expansion the method of self-similar approximants or Padé approximants, as discussed above, we get an approximant $\tau_k^*(t)$ whose limit, being by definition finite,

$$\tau_k^*(t) \to const \qquad (t \to \infty) \; ,$$

gives us the sought approximate expression for the relaxation time

$$\tau_k^* = \lim_{t\to\infty} \tau_k^*(t) \; . \tag{15}$$

Note that the value of the parameter A does not enter the consideration at all. In practice one can construct the approximants behaving as *const* for $t \to \infty$. The complete approximant for the sought function $\Phi(t)$ denoted as

Preprints (www.preprints.org) | NOT PEER-REVIEWED | Posted: 6 September 2020 doi:10.20944/preprints202009.0141.v1

$E(t,r)$ in can be constructed as well, or even some *ad hoc* forms satisfying some general symmetry can be applied, as in the Section 4.

As an illustration, let us find $\tau_k^*(t)$ in explicit form under some simple assumptions concerning its asymptotic behaviors. Assume simply that there are two distinct exponential behaviors for short and long times with two different τ_1, τ_2, and the transition from short to long time behavior also occur at the duration of some third characteristic time $\tau_3 = -\beta_3^{-1}$. The characteristic times can be found from the short-time expansion. The simple approximation to the effective relaxation time expressed in second order of (15), can be written down in the spirit of [7] as follows,

$$\tau_2{}^*(t)^{-1} = \beta_2 + (\beta_1 - \beta_2)\exp(\beta_3 t), \tag{16}$$

so that for negative β_3 we have $\tau_2^*(0)^{-1} = \beta_1$, $\tau_2^*(\infty)^{-1} = \beta_2$. In the theory of reliability the failure(hazard) rate or mortality force [8], are analogous to the inverse effective relaxation time, and the model of the type of formula (16) is known as Gompertz-Makeham law of mortality.

The complete approximant corresponding to (16) is reconstructed after elementary integration

$$F(t) = A\exp\left(\frac{(\beta_1 - \beta_2)\exp(\beta_3 t)}{\beta_3} + \beta_2 t\right), \tag{17}$$

with all unknown constituents of (16) expressed explictly, from the asymptotic equivalence with the power-series,

$$A = c_0\exp\left(\frac{\left({c_1}^2 - 2c_0c_2\right)^3}{4(3{c_0}^2c_3 - 3c_0{c_1}c_2 + {c_1}^3)^2}\right), \quad \beta_1 = \frac{c_1}{c_0}, \quad \beta_2 = \frac{6{c_0}^2c_1c_3 - 4{c_0}^2{c_2}^2 - 2c_0{c_1}^2c_2 + {c_1}^4}{2c_0(3{c_0}^2c_3 - 3c_0{c_1}c_2 + {c_1}^3)},$$
$$\beta_3 = \frac{2\left(3{c_0}^2c_3 - 3c_0{c_1}c_2 + {c_1}^3\right)}{c_0(2c_0c_2 - {c_1}^2)}. \tag{18}$$

Most interesting, as $\beta_2 = 0$, we arrive in different notations to the Gompertz function (101),

$$G(t) = A\exp\left(\frac{\beta_1\exp(\beta_3 t)}{\beta_3}t\right), \tag{19}$$

employed in calculations of [28]. In this case we have the effective relaxation time decaying exponentially with time. In the Section 4 we apply this method of finding the effective relaxation time for time series.

Preprints (www.preprints.org) | NOT PEER-REVIEWED | Posted: 6 September 2020 doi:10.20944/preprints202009.0141.v1

2.2 Critical index as control parameter. Optimization technique of self-similar root approximants

In order to understand the function's critical behavior, it is necessary to extrapolate the asymptotic expansion (1) to finite and even large values of the variable. Such an extrapolation can be accomplished by means of techniques just discussed above. But their successful application requires multi-termed expansions. How would it be possible to attempt and obtain reliable results for the critical indices employing a small number of terms in the asymptotic expansion? To this end we can employ the self-similar root approximants given by (103), where the external power m_k is to be determined from additional conditions. If the large-variable power α in equation (3) were known, then we could compare the latter with the large-variable behavior of the root approximant (103),

$$\mathcal{R}_k^*(x, m_k) \simeq A_k x^{km_k} \; , \tag{20}$$

where

$$A_k = (((\mathcal{P}_1^{m_1} + \mathcal{P}_2)^{m_2} + \mathcal{P}_3)^{m_3} + \ldots + \mathcal{P}_k)^{m_k} \; . \tag{21}$$

This comparison yields the relation $km_k = \alpha$, defining the external power $m_k = \frac{\alpha}{k}$, when α is known. This way of defining the external power is used when the root approximants are applied for interpolation. When several terms in the large-variable behavior are known, then the related powers define the values for the corresponding external powers m_j.

Consider the situation of exceptional difficulty where the large-variable behavior of the function is not known and α is not given. Moreover, the critical behavior can happen at a finite value x_c of the variable x. The direct method for calculating the critical index α by employing the technique of self-similar root approximants was developed in [50]. Suppose we construct several root approximants $R_k^*(x, m_k)$, in which the external power m_k plays the role of a control function. It is possible to treat the sequence $\{R_k^*(x, m_k)\}$ as a trajectory of a dynamical system, with the approximation order k playing the role of discrete time. A discrete-time dynamical system is called cascade, termed here the approximation cascade, since its trajectory consists of the sequence of approximants and the cascade velocity is defined by the general form of Euler discretization formula [53, 54, 55]

$$V_k(x, m_k) = \mathcal{R}_{k+1}^*(x, m_k) - \mathcal{R}_k^*(x, m_k) + (m_{k+1} - m_k) \frac{\partial}{\partial m_k} \mathcal{R}_k^*(x, m_k) \; . \tag{22}$$

Preprints (www.preprints.org) | NOT PEER-REVIEWED | Posted: 6 September 2020 doi:10.20944/preprints202009.0141.v1

The effective limit of the sequence $\{\mathcal{R}_k^*(x, m_k)\}$ corresponds to the fixed point of the cascade, where the cascade velocity tends to zero, as k tends to infinity. Having a finite number of approximants, the cascade velocity is not necessarily tending to zero, but certainly has to diminish for the sequence being convergent. Thus, the control functions $m_k = m_k(x)$, controlling convergence, are defined as the minimizers of the absolute value of the cascade velocity

$$|V_k(x, m_k(x))| = \min_{m_k} |V_k(x, m_k)| \; . \tag{23}$$

A finite critical point x_k^c, in the k-th approximation, exists if the equation

$$[\mathcal{R}_k^*(x_k^c, m_k)]^{1/m_k} = 0 \qquad (0 < x_k^c < \infty) \tag{24}$$

enjoys a finite solution for $x_k^c = x_k^c(m_k)$. Then the critical index in the k-th approximation is $\alpha_k = \lim_{x \to x_k^c} m_k(x)$. When we are studying the critical behavior at infinity, which we denote as $x_c \sim \infty$, keeping in mind that this case formally corresponds to the critical point at infinity, then the critical index is

$$\alpha = k \lim_{x \to \infty} m_k(x), \; as \; x_c \sim \infty \; . \tag{25}$$

Thus, the critical indices are defined, provided the control functions $m_k(x)$ are found. However, the minimization of the cascade velocity (98) poses some problems. First, equation (23) contains two control functions, m_{k+1} and m_k. Hence it is impossible to find two solutions from one equation. But it is possible to simplify the problem, when minimizing velocity (98), so that to get one equation for one control function. This can be done in two ways.

For instance, keeping in mind that m_{k+1} is close to m_k, equation (23) reduces to the *minimal difference condition*

$$\min_{m_k} \left| \mathcal{R}_{k+1}^*(x, m_k) - \mathcal{R}_k^*(x, m_k) \right| \qquad (k = 1, 2, \ldots) \; . \tag{26}$$

In particular, one can look for a solution $m_k = m_k(x)$ of the equation

$$\mathcal{R}_{k+1}^*(x, m_k) - \mathcal{R}_k^*(x, m_k) = 0 \; . \tag{27}$$

If the latter does not possess a solution for m_k, one has to return to (26). In general, when nothing is known on the form of the sought function $\Phi(x)$, the control functions m_k, depend on the variable x. But when we are looking for a function $\Phi(x)$ in the vicinity of its critical point x_c, where the function $\Phi(x)$

Preprints (www.preprints.org) | NOT PEER-REVIEWED | Posted: 6 September 2020 doi:10.20944/preprints202009.0141.v1

acquires critical form, the control functions are to be treated as the limits of $n_k(x)$ for $x \to x_c$. The control functions n_k, characterizing the critical behavior of $\Phi(x)$ become the numbers $m_k(x_c)$. In what follows, writing for short m_k, we assume $m_k = m_k(x_c)$.

Later in the Book, we also consider multiple examples when the complete control function $m_k(x)$, could be obtained analytically.

In the vicinity of a finite critical point, the function R_k^* behaves as

$$\mathcal{R}_k^*(x, m_k) \simeq \left(1 - \frac{x}{x_k^c}\right)^{m_k}, \; as \; x \to x_k^c - 0 \; . \tag{28}$$

Then condition (27) becomes

$$x_{k+1}^c(m_k) - x_k^c(m_k) = 0 \qquad (0 < x_k^c < \infty) \; . \tag{29}$$

When the critical behavior occurs at infinity, then it is convenient to introduce the control function

$$\mathsf{s}_k = k m_k \; , \tag{30}$$

so that the large-variable behavior of the root approximants reads as

$$\mathcal{R}_k^*(x, \mathsf{s}_k) \simeq A_k(\mathsf{s}_k) x^{\mathsf{s}_k}, \; as \; x \to \infty \; . \tag{31}$$

As a result, the minimal difference condition

$$\mathcal{R}_{k+1}^*(x, \mathsf{s}_k) - \mathcal{R}_k^*(x, \mathsf{s}_k) = 0 \tag{32}$$

leads to the equation

$$A_{k+1}(\mathsf{s}_k) - A_k(\mathsf{s}_k) = 0, \; as \; x_k^c \sim \infty \; . \tag{33}$$

The other equation for defining control functions follows from the minimal velocity condition (23), by remembering that $\mathcal{R}_{k+1}^*$ is close to $\mathcal{R}_k^*$, but usually m_{k+1} does not exactly coincide with m_k. Because of which one has to consider the minimal derivative condition

$$\min_k \left| \frac{\partial}{\partial m_k} \mathcal{R}_k^*(x, m_k) \right| \qquad (k = 1, 2, \ldots) \; . \tag{34}$$

In particular one can look for the solution of the equation

$$\frac{\partial}{\partial m_k} \mathcal{R}_k^*(x, m_k) = 0 \; . \tag{35}$$

Preprints (www.preprints.org) | NOT PEER-REVIEWED | Posted: 6 September 2020 doi:10.20944/preprints202009.0141.v1

However, the minimal derivative condition cannot be applied directly, when the sought function exhibits critical behavior, where the function either diverges or tends to zero. To apply this condition, it is necessary to extract from the function non-divergent parts. For example, if the critical point is finite, one can study the residue of the function $\partial \log \mathcal{R}_k^*/\partial m_k$, for which we have

$$\lim_{x\to x_k^c} (x_k^c - x)\, \frac{\partial}{\partial m_k}\, \log \mathcal{R}_k^*(x, m_k) = m_k\, \frac{\partial x_k^c}{\partial m_k}\ .$$

Thus, instead of equation (35), we get the condition

$$\frac{\partial x_k^c}{\partial m_k} = 0 \qquad (0 < x_k^c < \infty)\ . \tag{36}$$

When the critical behavior occurs at infinity, then we can consider the limit

$$\lim_{x\to\infty} \frac{\mathcal{R}_k^*(x, \mathsf{s}_k)}{x^{\mathsf{s}_k}} = A_k(\mathsf{s}_k)\ ,$$

for which equation (35), defining control functions, reduces to the form

$$\frac{\partial A_k(\mathsf{s}_k)}{\partial \mathsf{s}_k} = 0,\ as\ x_k^c \sim \infty\ . \tag{37}$$

Let us consider the widely studied case of the two-dimensional channel bounded by the surfaces $z = \pm b\ (1 + \varepsilon \cos x)$, where ε is termed *waviness*. The permeability possesses the critical behavior [11], when (in the case of $b = 0.5$) it tends to zero as

$$K(\varepsilon) \sim (\varepsilon_c - \varepsilon)^{\varkappa},\ \text{as}\ \varepsilon \to \varepsilon_c - 0\ , \tag{38}$$

with $\varepsilon_c = 1$, $\varkappa = \frac{5}{2}$. An expression for permeability as a function of the waviness parameter can be derived by perturbation theory in the form of an expansion in powers of the waviness [11, 13]. The permeability, for $b = 0.5$, has the expansion

$$K(\varepsilon) \simeq 1 - 3.14963\ \varepsilon^2 + 4.08109\ \varepsilon^4,\ \text{as}\ \epsilon \to 0\ . \tag{39}$$

With our method, setting $\varepsilon_c = 1$, and using the change of the variable $y = \frac{\varepsilon^2}{1-\varepsilon^2}$, one shifts the critical point to infinity. Then, the critical index is calculated as explained above and in [50], giving from the minimal-difference condition $\varkappa_1 = 2.184$, with an error 12.6%, and from the minimal derivative condition $\varkappa_2 = 2.559$, with an error 2.37%.

Preprints (www.preprints.org) | NOT PEER-REVIEWED | Posted: 6 September 2020 doi:10.20944/preprints202009.0141.v1

The final answer can be presented as the average [50]

$$\varkappa^* = \frac{1}{2}\left(\varkappa_1 + \varkappa_2\right) \pm \frac{1}{2}\left|\varkappa_1 - \varkappa_2\right| ,$$

and we find $\varkappa^* = 2.372 \pm 0.19$.

The permeability, for $b = 0.25$, has the expansion

$$K(\varepsilon) \simeq 1 - 3.03748\,\varepsilon^2 + 3.54570\,\varepsilon^4, \ \text{as} \ \varepsilon \to 0 . \tag{40}$$

Setting $\varepsilon = 1$, and using the same change of the variable as above, the critical index is found, so that $\varkappa_1 = 2.342$, and $\varkappa_2 = 2.743$. Thus, we have $\varkappa^* = 2.543 \pm 0.2$.

We also illustrate the numerical convergence of root approximants in high-orders, when applied for calculating critical indices. As an example, we consider the same two cases of permeability $K(\varepsilon)$, but with higher-order terms included, limited to the 16th order terms inclusively. The numerical values of the corresponding coefficients can be found in Section 3, see expansion (56), and expansion (65). Namely, we construct the root approximants

$$\mathcal{R}_k^*(y) = \left(\left(\left((1 + \mathcal{P}_1 y)^2 + \mathcal{P}_2 y^2 \right)^{3/2} + \mathcal{P}_3 y^3 \right)^{4/3} + \ldots + \mathcal{P}_k y^k \right)^{\alpha/k} , \tag{41}$$

defining the parameters $\mathcal{P}_j$ from the asymptotic equivalence procedure. This gives the permeability the following asymptotic forms

$$\mathcal{R}_k^*(y) \simeq A_k y^{\alpha}, \ as \ y \to \infty , \tag{42}$$

where the amplitudes $A_k = A_k(\alpha_k)$ are

$$A_k = \left(\left((\mathcal{P}_1^2 + \mathcal{P}_2)^{3/2} + \mathcal{P}_3 \right)^{4/3} + \ldots + \mathcal{P}_k \right)^{\alpha/k} . \tag{43}$$

In order to define the critical index α_k, we analyze the differences

$$\Delta_{kn}(\alpha_k) = A_k(\alpha_k) - A_n(\alpha_k) . \tag{44}$$

Composing the sequences $\Delta_{kn} = 0$, we find the related approximate values α_k for the critical indices. It is possible to investigate different sequences of the conditions $\Delta_{kn} = 0$, the most logical from which are the sequences of $\Delta_{k,k+1} = 0$ and of $\Delta_{k8} = 0$, with $k = 1, 2, 3, 4, 5, 6, 7$. The results, presented in Table

Preprints (www.preprints.org) | NOT PEER-REVIEWED | Posted: 6 September 2020 doi:10.20944/preprints202009.0141.v1

$\varkappa_k$	$\Delta_{k+1}(\varkappa_k)=0$	$\Delta_{k8}(\varkappa_k)=0$
$\varkappa_1$	2.18445	2.39678
$\varkappa_2$	2.68311	2.52028
$\varkappa_3$	2.48138	2.49208
$\varkappa_4$	2.49096	2.49692
$\varkappa_5$	2.5012	2.49982
$\varkappa_6$	2.49935	2.499
$\varkappa_7$	2.49861	2.49861

Table 1: Case of b=1/2. Critical indices for the permeability $\varkappa_k$ obtained from the optimization conditions $\Delta_{kn}(\varkappa_k)=0$. The sequences demonstrate numerical convergence to the value $\varkappa=5/2$.

$\varkappa_k$	$\Delta_{k+1}(\varkappa_k)=0$	$\Delta_{k8}(\varkappa_k)=0$
$\varkappa_1$	2.34165	2.452
$\varkappa_2$	2.52463	2.50542
$\varkappa_3$	2.4976	2.49933
$\varkappa_4$	2.49941	2.50004
$\varkappa_5$	2.50028	2.50033
$\varkappa_6$	2.50032	2.50036
$\varkappa_7$	2.50041	2.50041

Table 2: Case of b=1/4. Critical indices for the permeability $\varkappa_k$ obtained from the optimization conditions (44),$\Delta_{kn}(\varkappa_k)=0$. The sequences of α_k demonstrate good numerical convergence to the value $\varkappa=5/2$.

Preprints (www.preprints.org) | NOT PEER-REVIEWED | Posted: 6 September 2020 doi:10.20944/preprints202009.0141.v1

ν_k	$\Delta_{k+1}(\nu_k)=0$	$\Delta_{k8}(\nu_k)=0$
ν_1	-6	-4.36
ν_2	-4.04	-4.1
ν_3	n.a.	-4.13
ν_4	-4.09	-4.05
ν_5	-3.97	-4.03
ν_6	n.a.	-4.08
ν_7	-3.94	-3.94

Table 3: Case of b=1/2. Walls can not touch. Critical indices for the permeability for the problem of Section 3, subsection 3.1.3, obtained from the optimization conditions $\Delta_{kn}(\nu_k)=0$. The sequences demonstrate reasonably good numerical convergence to the value $\nu=-4$.

1 (for $b=\frac{1}{2}$), show good numerical convergence of the approximate critical indices $\alpha_k \equiv \varkappa_k$ in our case, to the exact value $\varkappa=\frac{5}{2}$. Similarly, the results, presented in Table 2 (for $b=\frac{1}{4}$), again demonstrate rather good numerical convergence of the approximate critical indices to the exact value. The value of critical index does not depend on parameter b. The sequence, based on the *DLog* Padé method, is convergent as well, and results in consistent physical solutions, see the next Section 3.

Consider yet different case of permeability $K(\varepsilon)$, see Section 3, subsection 3.1.3. For the parallel sinusoidal two-dimensional channel there is no possibility of the walls touching, and permeability remains finite but expected to decay as a power-law as ε becomes large. In the expansion of $K(\varepsilon)$ in small parameter ε^2 we retain the terms up the 16th order terms inclusively. The numerical values of the corresponding coefficients can be found in Section 3, see expansion (68) on page 28. In this case, the permeability decays as

$$K(\varepsilon) \sim \varepsilon^{\nu}, \text{ as } \varepsilon \to \infty,$$

with negative index ν. Results of calculations are presented in Table 3 (for $b=\frac{1}{2}$), and show good numerical convergence, especially in the last column, to the value -4. The sequence, based on the *DLog* Padé method, is convergent as well, see Section 3, subsection 3.1.3.

 doi:10.20944/preprints202009.0141.v1

3 Critical permeability

Quantitative understanding of processes that govern flow and transport in porous and discontinuous media is of utmost importance in many geophysical processes. For instance, the presence of fluid is one of the leading candidate to solve a variety of paradoxes in the physics of earthquakes such as the apparent weakness of mature faults. Understanding the transport properties of fluids in the fragmented crust in the presence of discontinuities occurring at many length scales is an essential component in the ultimate goal of understanding earthquakes. Understanding the properties of transport of fluids in complex porous and cracked media at many scales is also of fundamental importance from an environmental point of view as well as for the storage of contaminants or pollutants or to remedy sites from contamination. The theory of porous and fractured porous media is widely applicable to engineering problems of oil industry.

Critical behavior of permeability of certain, power-series- treatable models of Darcy flow in porous media is studied in this section. Permeability of spatially periodic arrays of cylinders was found in an analytical form in [9]. Transverse flow past hexagonal and square arrays of cylinders were studied as well, based on expansions for small concentrations and lubrication approximation for high concentrations of cylinders [9]. 3D periodic arrays of spherical obstacles are discussed in [9] as well. Formulas for the drag force exerted by various lattices of obstacles are derived from the low-concentration expansions.

Below, the Stokes flow through a 2D and 3D channels enclosed by two wavy walls is studied by means of the analytical-numerical algorithm. Efficient formulas for the permeability are derived in the form of series for small values of amplitude. Various power-laws are found in the regime of large amplitudes, based only on expansions at small amplitudes. Lubrication approximation is shown to break down, but an accurate formulas for the effective permeability for arbitrary values of the wave amplitude are derived from the expansions.

This section deals exclusively with constructive analytical solutions. In other words with approximate analytical solutions, when the resulting formulas contain the main physical and geometrical parameters. The available truncated series are considered as polynomials. They remember their infinite expansions, so that with a help of some additional resummation procedure one can extrapolate to the whole series by means of special constructive forms

 doi:10.20944/preprints202009.0141.v1

called approximants, that are asymptotically equivalent to the truncated series. The approximants are richer than original polynomials in a sense that they also suggest an infinite additional number of the coefficients. The quality of approximants significantly improves when more than one asymptotic regime can be studied and incorporated into the approximant.

For low Reynolds numbers $\mathcal{R}$, the flow of a viscous fluid through a channel is described by the well-known Darcy's law which corresponds to a linear relation between the pressure gradient $\overline{\nabla p}$ and the average velocity $\overline{u}$ along the pressure gradient [11]

$$|\overline{\nabla p}| = \frac{\eta}{K}\overline{u}, \tag{45}$$

where K is the permeability and η is the dynamic viscosity of the fluid. The permeability characterizes the amount of viscous fluid flow through a porous medium per unit time and unit area when a unit macroscopic pressure gradient is applied to the system. The classical Poiseuille flow in the channel bounded by two parallel planes separated by a distance $2b$, generated by an average pressure gradient $\overline{\nabla p}$ is a classic example which yields the Darcy's law. The flow profile is parabolic when the Reynolds number R is small.

When the channel is not straight and when the Reynolds number is not negligible, additional terms appear in this relation [13, 12]. Yet Darcy law holds for the Stokes flow through a channel with three-dimensional wavy walls enclosed by two wavy walls whose amplitude is proportional to the mean clearance of the channel multiplied by the small dimensionless parameter ε. Mind that special technology used for stimulation of petroleum wells leads to the formation of highly conductive channels, so-called wormholes. The channel can be just a single conduit with a minimum of branching. It seems feasible to represent the wormhole by a wavy-walled channel. Channels can be considered jointly as a network of one-dimensional channels. The permeability of a single channel models the permeability of the corresponding edge in the network. Application of the standard methods of flows in networks yields the macroscopic permeability of the considered media. The ultimate result essentially depends on the graph, modeling the network.

Another problem when Darcy low does hold, corresponds to the longitudinal or transverse permeability of a spatially periodic square or hexagonal array of circular cylinders, when a Newtonian fluid is flowing at low Reynolds number along and perpendicular to the cylinders. Non of the currently available expressions for the transverse permeability can be considered satisfactory simultaneously in both, high-and-low porosity limits. The problems of

Preprints (www.preprints.org) | NOT PEER-REVIEWED | Posted: 6 September 2020 doi:10.20944/preprints202009.0141.v1

permeability and conductivity belong to two different classes [10], for small and moderate volume fractions mathematical structure of the permeability problem is Laplacian, and can be addressed by the same methodology as conductivity. But for high volume fractions, such reduction does not work, since it appears that problems of permeability and conductivity are characterized by different critical exponents.

Darcy low also is prerequisite for lattice and continuum percolation models, used to predict critical behavior of the fluid permeability. A random pipe network is a generic model of percolation. It is equivalent to a random resistor network, and is used to simulate fluid flow in the vital case of a sea ice, with a profound implications for Climate [14, 15]. Even possibility is being considered to to repair the Ice Sheet Instability by constructing either a continuous artificial sill, or finding isolated artificial pinning points to counter a collapse [17].

The fluid permeability $K(f)$ of random network, where f stands for the pipe/bond fraction, is the ratio between the macroscopic fluid current density and the applied pressure gradient. The bonds could be interpreted as open or closed pipes, and the permeability follows the power-law in the vicinity of a percolation threshold f_c, $K(f) \sim (f - f_c)^{\varkappa}$, where $\varkappa$ is the fluid permeability exponent [10].

Consider a discrete lattice percolation. Usually, it is tacitly assumed that the target random structure is obtained from the uniform identical distribution of bonds. This corresponds to the "complete stirring" in the James Bond paradigm [2]. Though different authors use theoretically same uniform identical distribution, it is known that the ultimate result can depend on the simulation protocol. We suppose that the discussed results were obtained on the basis of the same theoretical model and similar protocols, i.e., we assume that the same "game of chance" was played. Under acceptance of such rules concerning the structure of media, one believes that $\varkappa = \mathsf{t}$, where t is the conductivity critical exponent. For lattices the index t is believed to be universal, depending only on space dimensions. In 2D, $\mathsf{t} \approx 1.3$, and in 3D, $\mathsf{t} \approx 2.0$. Thus, the critical index is determined by analogy and from numerical experimentation. Although continuum models can exhibit a non-universal behavior, with the critical exponent values different from the lattice case. A rough estimate for the fluid permeability critical exponent $\varkappa$ for sea ice, is about 2.5 [14]. Strikingly, the two classical models mentioned above based on direct hydrodynamic solutions, also demonstrate power-law behavior around their corresponding thresholds, with the very same value

Preprints (www.preprints.org) | NOT PEER-REVIEWED | Posted: 6 September 2020 doi:10.20944/preprints202009.0141.v1

of the critical exponent 5/2! Mind that the permeability exponent for the Swiss cheese model of continuum percolation was determined numerically to be close with the value of 2.53 [16]. Thus, reality places obvious limitations on application of pure lattice percolation models, but stresses the necessity to study critical phenomena directly from the hydrodynamic equations to deduce transport coefficients via homogenization procedure. If the transport medium is taken as empty space where viscous fluid can flow through, and the cylinders are taken as solid phase blocking the fluid, one still encounters the critical exponent describing the behavior of fluid permeability K near the threshold for the flow. But in the cases considered below in this section, the critical exponent can be calculated directly from the solution of Stokes problem.

3.1 Permeability in wavy-walled channels

In Ref. [13] a general asymptotic analysis was applied to a Stokes flow in curvilinear three-dimensional channels bounded by walls of the form

$$z = S^{+}(x_1, x_2) \equiv b\big(1 + \varepsilon T(x_1, x_2)\big), \tag{46}$$

$$z = S^{-}(x_1, x_2) \equiv -b\big(1 + \varepsilon B(x_1, x_2)\big). \tag{47}$$

In what follows, the formally small dimensionless parameter $\varepsilon \geq 0$ is employed to present the form (46) as the perturbation around the straight channel.

Such approach generalizes an original Pozrikidis work on two-dimensional channels [18]. Recently, this approach was extended to the gravity driven Stokesian flow past the wavy bottom [19, 20], to wavy tubes [21] and to the Navier-Stokes equations [12, 22], to the stationary heat conduction [23], to electrokinetic phenomena in two-dimensional channels [24]. An arbitrary profiles $S^{\pm}(x_1, x_2)$ were considered, satisfying some natural conditions. For definiteness, it was assumed that

$$|T(x_1, x_2)| \leqslant 1 \quad \text{and} \quad |B(x_1, x_2)| \leqslant 1. \tag{48}$$

For an infinitely differentiable $T(x_1, x_2)$ and $B(x_1, x_2)$, in order to calculate velocities and permeability, one has to solve a cascade of boundary value problems for the Stokes equations for a straight channel [13]. Influence of curvilinear edges on flow is of fundamental interest since it illustrates the

Preprints (www.preprints.org) | NOT PEER-REVIEWED | Posted: 6 September 2020 doi:10.20944/preprints202009.0141.v1

mechanism of viscous flow under different geometrical conditions. Apart from its theoretical importance, the flow through curvilinear channels has application in porous media [11, 25].

General expression for permeability as a function of ε can be deduced and the limiting value when eddies arise can be estimated as well. Application of the method of perturbation on ε turned out to be an efficient way to solve the problem, i.e. to calculate velocities and permeability in the form of an ε–expansion.

Let $\mathbf{u} = \mathbf{u}(x_1, x_2, x_3)$ be the velocity vector, and $p = p(x_1, x_2, x_3)$ the pressure. The flow of a viscous fluid through a channel is considered under the assumption that the Reynolds number is small enough for Stokes flow approximation to be made. Thus the fluid is governed by the Stokes equations

$$\begin{aligned} &\mu\nabla^2\mathbf{u} = \nabla p, \\ &\nabla\cdot\mathbf{u} = \mathbf{0} \end{aligned} \tag{49}$$

with the boundary conditions

$$\mathbf{u} = \mathbf{0} \qquad \text{on} \quad S^{\pm}. \tag{50}$$

The solution $\mathbf{u}$ of (49)–(50) belongs to the class of periodic functions with period $2L$ in x_1 and x_2.

Let also u be the x-component of $\mathbf{u}$. Apply an overall external gradient pressure $\overline{\nabla p}$ along the x_1-direction. It can be described by a constant jump $2L\overline{\nabla p}$ along the x_1-axis of the periodic cell. The permeability of the channel in the x_1-direction is defined as follows

$$K_{x_1}(\varepsilon) = -\frac{\mu}{\overline{\nabla p}\,|\tau|}\int_{-L}^{L}\int_{-L}^{L} dx_1\,dx_2 \int_{S^-(x_1,x_2)}^{S^+(x_1,x_2)} u(x_1, x_2, x_3)\,dx_3\,, \tag{51}$$

where $|\tau|$ is the volume of the unit cell Q of the channel,

$$|\tau| = \int_{-L}^{L}\int_{-L}^{L} dx_1\,dx_2 \int_{S^-(x_1,x_2)}^{S^+(x_1,x_2)} dx_3\,. \tag{52}$$

$K_{x_1}(\varepsilon)$ in (51) is considered as a function in ε. For convenience the ratio $K = K(\varepsilon)$ of the dimensional permeability for the curvilinear channel and of

Preprints (www.preprints.org) | NOT PEER-REVIEWED | Posted: 6 September 2020 doi:10.20944/preprints202009.0141.v1

the Poiseuille flow

$$K(\varepsilon) = \frac{K_{x_1}(\varepsilon)}{K_{x_1}(0)}, \tag{53}$$

is considered. The case $\varepsilon = 0$ corresponds to the well-known Poiseuille flow, for which (51) yields the permeability

$$K_{x_1}(0) = \frac{b^2}{3}, \tag{54}$$

as the flow profile in this limit-case obeys the parabolic law.

More precisely, the formula derived in [13] determines the coefficients of a Taylor expansion for the permeability

$$K(\varepsilon) = \sum_{m=0}^{\infty} c_m \varepsilon^m.$$

and normalization (53) is used for K. In practical computations $K(\varepsilon)$ is approximated by the Taylor polynomial

$$K_N(\varepsilon) = \sum_{m=0}^{N} c_m \varepsilon^m.$$

The domain of application of this formula is restricted, since the corresponding Taylor series can be divergent for larger ε.

3.1.1 Symmetric sinusoidal two-dimensional channel. Breakdown of lubrication approximation

Let us consider the two-dimensional channel bounded by the surfaces

$$z = b(1 + \varepsilon \cos x) \quad , \quad z = -b(1 + \varepsilon \cos x). \tag{55}$$

The permeability was calculated up to $O(\varepsilon^{32})$, for $b = 0.5$. This example is typical among the references cited in [13]. The following series for permeability as the function of "waviness" parameter where obtained,

$$\begin{aligned} &K_{30}(\varepsilon) = \\ &1 - 3.14963\varepsilon^2 + 4.08109\varepsilon^4 - 3.48479\varepsilon^6 + 2.93797\varepsilon^8 - 2.56771\varepsilon^{10} + \\ &2.21983\varepsilon^{12} - 1.93018\varepsilon^{14} + 1.67294\varepsilon^{16} - 1.45302\varepsilon^{18} + 1.26017\varepsilon^{20} - \\ &1.09411\varepsilon^{22} + 0.949113\varepsilon^{24} - 0.823912\varepsilon^{26} + 0.714804\varepsilon^{28} - 0.620463\varepsilon^{30} \\ &+O(\varepsilon^{32}). \end{aligned} \tag{56}$$

Preprints (www.preprints.org) | NOT PEER-REVIEWED | Posted: 6 September 2020 doi:10.20944/preprints202009.0141.v1

A lubrication approximation in the case of two cylinders of different radii that are almost in contact with one another along a line was discussed in [11]. For equal radii a, the flow rate q per unit length is proportional to the pressure variation Δp

$$q = -\frac{K_l}{\mu}\Delta p, \tag{57}$$

where K_l is given by

$$K_l = \frac{2}{9\pi}\sqrt{\frac{\delta^5}{a}} \tag{58}$$

and δ is the gap between the cylinders.

For the channel (55), if ε is close to unity, the aperture at $x = -\pi$ is close to zero. Hence, one can apply (58) to this local channel with $\delta = 2b(1-\varepsilon)$ and $a = b\varepsilon$. As $\varepsilon \to \varepsilon_c = 1$, one would simply have the following expression,

$$K_l \simeq \frac{8\sqrt{2}\sqrt{b^4}(\varepsilon-1)^{5/2}}{9\pi}, \tag{59}$$

which matches the general critical form with the critical index for permeability $\varkappa = 5/2$, and the critical amplitude $A = \frac{8\sqrt{2}b^2}{9\pi}$. Thus, in the case under consideration $A = 0.100035$.

The lubrication approximation [11] considers situations when the amplitude of the wall oscillations is smaller than the channel width [26]. It also turns out that the channel width should be small when compared to a characteristic length of the channel, i.e., $\varepsilon \ll b \ll 2\pi$. The main assumption of the lubrication approximation is that the velocity has a parabolic profile. It is demonstrated for the plane channels [13], that lubrication approximation gives correct results only for channels in which the mean surface

$$S(x_1, x_2) = b + \frac{\varepsilon}{2}\big(T(x_1, x_2) - B(x_1, x_2)\big)$$

is sufficiently close to a plane and for small value of ε.

Our main goal is to avoid using the lubrication approximation and find the way to approach the critical region (walls nearly touch) only based on (56).

The problem of interest can be formulated mathematically as follows. Given the polynomial approximation (56) of the function $K(\varepsilon)$, to determine critical index and amplitude(s) of the asymptotically equivalent approximation near $\varepsilon = \varepsilon_c = 1$. When such extrapolation problem is solved, we proceed to solve an interpolation problem, assuming that the critical behavior

Preprints (www.preprints.org) | NOT PEER-REVIEWED | Posted: 6 September 2020 doi:10.20944/preprints202009.0141.v1

is known in advance and derive the compact formula for all ε. Let us look for the critical behavior in general form

$$K(\varepsilon) \simeq A(\varepsilon_c - \varepsilon)^{\varkappa}, \text{ as } \varepsilon \to \varepsilon_c - 0 \,, \tag{60}$$

and calculate the index and amplitude.

It is clear how to proceed routinely with critical index calculations when the value of the threshold is known. One would first apply the following transformation,

$$z = \frac{\varepsilon}{1-\varepsilon} \;\Leftrightarrow\; \varepsilon = \frac{z}{z+1},$$

to the series (56) in order to make application of the different approximants more convenient.

Then, to such transformed series $M_1(z)$ apply the $DLog$ transformation (differentiate Log of $M_1(z)$) and call the transformed series $M(z)$. In terms of $M(z)$ one can readily obtain the sequence of approximations $\varkappa_n$ for the critical index $\varkappa$,

$$\varkappa_n = -\lim_{z\to\infty}(zPadeApproximant[M[z], n, n+1]). \tag{61}$$

There is an excellent convergence within the approximations for the critical index generated by the sequence of Padé approximants, corresponding to their order increasing to the value $5/2$:

$$\varkappa_1 = 2.57972, \quad \varkappa_2 = 2.30995, \quad \varkappa_3 = 2.47451, \quad \varkappa_4 = 2.49689,$$

$$\varkappa_5 = 2.4959, \quad \varkappa_6 = 2.49791, \quad \varkappa_7 = 2.49923, \quad \varkappa_8 = 2.50113,$$

$$\varkappa_9 = 2.50028, \varkappa_{10} = 2.49783, \varkappa_{11} = 2.49778, \varkappa_{12} = 2.49829, \varkappa_{13} = 2.49836.$$

If $B_n(z) = PadeApproximant[M[z], n, n+1]$, then

$$K_n^*(\varepsilon) = \exp\left(\int_0^{\frac{\varepsilon}{\varepsilon_c-\varepsilon}} B_n(z)\, dz\right), \tag{62}$$

and one can compute numerically corresponding amplitude

$$A_n = \lim_{\varepsilon\to\varepsilon_c}(\varepsilon_c - \varepsilon)^{-\varkappa_n} K_n^*(\varepsilon), \tag{63}$$

with $A_9 = 3.7758$, by order of magnitude larger than the value anticipated from the lubrication. With critical index fixed to $5/2$, one can calculate A using standard Padé technique, leading to the very close value of 3.77188.

Preprints (www.preprints.org) | NOT PEER-REVIEWED | Posted: 6 September 2020 doi:10.20944/preprints202009.0141.v1

In the compact form permeability can be expressed in terms of factor approximant, which is asymptotically equivalent to (56) up to 16th order inclusively,

$$K^*_{1/2}(\varepsilon) = \frac{\left(1-\varepsilon^2\right)^{2.5}\left(0.239311\varepsilon^2+1\right)^{0.591597}}{(1-0.722851\varepsilon^2)^{0.00840612}(1-0.260764\varepsilon^2)^{0.270545}(0.867799\varepsilon^2+1)^{1.00004}}, \qquad (64)$$

with amplitude $A = 3.77177$. Mind that there are "spare", higher order coefficients, not employed in construction of (64). The maximal error in reproducing these higher-order coefficients defines the accuracy of the studied crossover formula. From the formula (64) one can readily obtain the higher-order coefficients (56), not employed in the final formula,

$$c_{18} = -1.453, \quad c_{20} = 1.26014, \quad c_{22} = -1.09408, \quad c_{24} = 0.949078,$$
$$c_{26} = -0.823874, \quad c_{28} = 0.714764, \quad c_{30} = -0.620422.$$

Formula (64) appears to be exceptionally accurate in reproducing the coefficients in the expansion (56) not employed in its construction. The maximal error appears in reproducing the $30th$ order, and it equals just 0.0066%. Similar problem is important also in quantum field theory, and was formulated by Richard Feynman. Feynman hoped that in perturbative theories it would be possible to estimate the result for the coefficient in a given order, without the brute force evaluation of all the diagrams contributing in this order. The complexity of calculations increases very rapidly in high orders, and even a way of determining the sign of the contribution would be useful.

We conclude that the lubrication approximation breaks down even in a close vicinity of ε_c, as anticipated in [13]. In figure 1 formula (64) is compared with the asymptotic regimes. Note that lubrication theory gives correct estimate for the critical index.

3.1.2 Symmetric sinusoidal two-dimensional channel. Breakdown-example 2

Let us consider now the channel bounded by the surfaces (55) with $b = 0.25$. $K(\varepsilon)$ was obtained in [13],

$$\begin{aligned} &K(\varepsilon) = \\ &1 - 3.03748\varepsilon^2 + 3.54570\varepsilon^4 - 2.33505\varepsilon^6 + 1.35447\varepsilon^8 - 0.83303\varepsilon^{10} \\ &+0.49762\varepsilon^{12} - 0.30350\varepsilon^{14} + 0.18185\varepsilon^{16} - 0.11083\varepsilon^{18} + 0.06636\varepsilon^{20} \\ &-0.04051\varepsilon^{22} + 0.02419\varepsilon^{26}0.00880\varepsilon^{28} - 0.00544\varepsilon^{30} + \\ &O(\varepsilon^{32}). \end{aligned} \qquad (65)$$

Preprints (www.preprints.org) | NOT PEER-REVIEWED | Posted: 6 September 2020 doi:10.20944/preprints202009.0141.v1

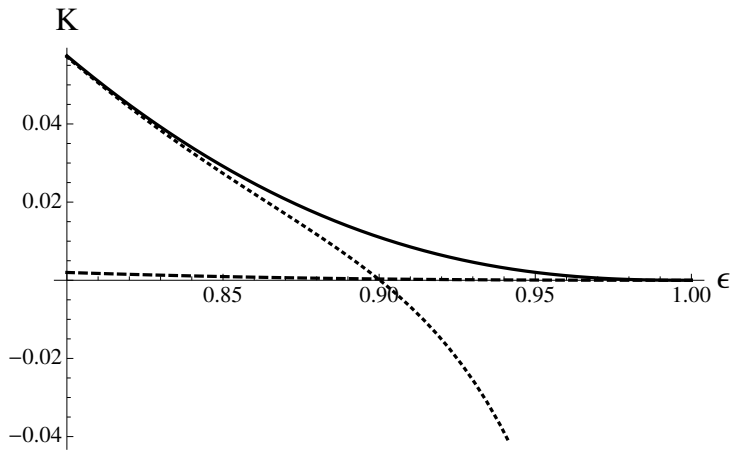

Figure 1: Formula (64) (solid) is compared with the power series (dotted) and lubrication approximation (dashed)

There is an excellent convergence within the approximations for the critical index generated by the sequence of Padé approximants, corresponding to their order increasing:

$$\varkappa_1 = 2.64456, \quad \varkappa_2 = 2.41346, \quad \varkappa_3 = 2.49488, \quad \varkappa_4 = 2.49992,$$
$$\varkappa_5 = 2.49991, \quad \varkappa_6 = 2.50026, \quad \varkappa_7 = 2.50068, \quad \varkappa_8 = 2.50087,$$
$$\varkappa_9 = 2.50086, \quad \varkappa_{10} = 2.50063, \quad \varkappa_{11} = 2.50063, \quad \varkappa_{12} = 2.50086,$$
$$\varkappa_{13} = 2.50087, \quad \varkappa_{14} = 2.50068, \quad \varkappa_{15} = 2.50026.$$

Evidently this sequence implies the same value for the index, $\varkappa = 5/2$. The value of amplitude is estimated by $A_{15} = 3.77362$. Both amplitude and index are in complete agreement with the results for different b obtained above.

With critical index fixed to $5/2$, one can calculate the amplitude A, using standard Padé technique, leading to the very close value of $A \approx 3.77316$. In the compact form permeability can be expressed through the following factor approximant

$$K^*_{1/4} = \frac{(1-\varepsilon^2)^{2.5}}{(1-0.0437141\varepsilon^2)^{1.37166}\,(0.606745\varepsilon^2+1)^{0.984665}}, \tag{66}$$

with amplitude calculated as $A = 3.77062$. This value is by orders of magnitude different from the value 0.02501, suggested by the lubrication theory.

Preprints (www.preprints.org) | NOT PEER-REVIEWED | Posted: 6 September 2020 doi:10.20944/preprints202009.0141.v1

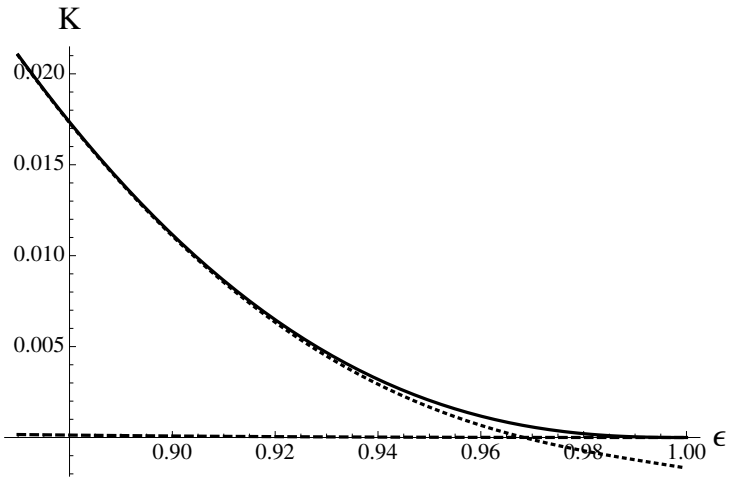

Figure 2: Formula (66) (solid) is compared with the power series (dotted) and lubrication approximation (dashed)

From the crossover formula (66) one can readily obtain the higher-order coefficients (65), not employed in the derivation,

$$c_{10} = -0.833087, \quad c_{12} = 0.497914, \quad c_{14} = -0.304065, \quad c_{16} = 0.1825,$$

$$c_{18} = -0.111442, \; c_{20} = 0.0668887, \; c_{22} = -0.0409299, \; c_{24} = 0.0245076,$$

$$c_{26} = -0.0150614, \quad c_{28} = 0.00896906, \quad c_{30} = -0.00555677.$$

Formula (64) appears to be accurate in reproducing the coefficients in the expansion (56), even not employed in its construction. The maximal error is in reproducing c_{30}, and it is equal to 2.147%.

In figure 2 formula (66) is compared with the asymptotic regimes. Note that lubrication theory gives correct estimate for the critical index. The amplitude and overall behavior of permeability in the vicinity of ε_c, practically does not depend on the parameter b. One can think that some universal (not dependent on b) mechanism is at work here, the chief suspect being celebrated similarity-solutions with complex exponent, known as viscous Moffat eddies [27], obviously not covered by the lubrication theory [26]. Eddies manifest themselves as reversed-flow regions near the walls. Onset of eddies is expected in the vicinity of ε_e, corresponding to zero of the polynomial approximations (64), (66), and would lead to a total disappearance of permeability, an artifact being corrected by a detailed consideration of the region

Preprints (www.preprints.org) | NOT PEER-REVIEWED | Posted: 6 September 2020 doi:10.20944/preprints202009.0141.v1

$\varepsilon \sim 1$ with a power-law ansatz. As value of b decreases, the value of ε_e moves closer to ε_c.

Due to Moffat it is understood that steady two-dimensional low-Reynolds number sharp corner flow between two fixed plane rigid boundaries has a remarkably universal form. The motion is being driven by some arbitrary stirring mechanism far from the corner. We largely follow Moffat's brilliant, somewhat poetic description of the eddies. The stream function ought to satisfy the biharmonic equation which has only complex solutions. The velocity components appear to oscillate infinitely albeit quite strongly damped, implying the existence of an infinitely reversing sequence of eddies as the corner is approached. The solution is truly universal, providing the asymptotic form of the generic two-dimensional flow near any sharp corner, irrespective of the nature of the remote forcing. Even if the remote flow conditions are in the high-Reynolds-number regime, the local Reynolds number near any perfectly sharp corner is always small, so that the low-Reynolds-number eddies are always present, but on an extremely small scale in the immediate vicinity of the corner! It is, however, quite clear that, although the mathematics implies an infinite geometrical sequence of eddies, not more than two or three of these eddies will ever be observed in practice. In reality the corner may be not quite sharp, in which case the infinite sequence of eddies is simply replaced by a finite sequence, the number depending in an obvious way on the degree of rounding of the corner. It appears that the tiny corner eddies, too weak to be observed under steady conditions, do play a role when the remote conditions are time-periodic: they emerge successively from the corner, one in each half-period, growing in stature like Kabuki actors on a stage, and ultimately taking the lead role [27].

3.1.3 Parallel sinusoidal two-dimensional channel. Novel critical index

The present channel is bounded by the surfaces

$$z = b(1 + \varepsilon \cos x) \ , \quad z = -b(1 - \varepsilon \cos x) \ , \tag{67}$$

with $b = 0.5$. There is no possibility of the walls touching and permeability remains finite but expected to decay as a power-law as ε becomes large. Instead of a critical transition from permeable to non-permeable phase, we have a non-critical transition, or crossover from high-to low permeability with increasing parameter ε. The crossover can be still characterized by the

Preprints (www.preprints.org) | NOT PEER-REVIEWED | Posted: 6 September 2020 doi:10.20944/preprints202009.0141.v1

power-law, and corresponding index at large ε. There is no eddy in such channel even for very large ε, and lubrication approximation does not work at all [13]. For large b eddies are not excluded.

The permeability is calculated up to $O(\varepsilon^{32})$,

$$\begin{aligned}
&K_{30}(\varepsilon) = \\
&1 - 2.53686\times10^{-1}\varepsilon^2 + 4.28907\times10^{-2}\varepsilon^4 - 5.46188\times10^{-3}\varepsilon^6 \\
&+4.54695\times10^{-4}\varepsilon^8 + 9.0656\times10^{-6}\varepsilon^{10} - 1.41572\times10^{-5}\varepsilon^{12} + 3.76584\times10^{-6}\varepsilon^{14} \\
&-6.72021\times10^{-7}\varepsilon^{16} + 7.58331\times10^{-8}\varepsilon^{18} + 2.34495\times10^{-9}\varepsilon^{20} - 4.59993\times10^{-9}\varepsilon^{22} \\
&+1.88446\times10^{-9}\varepsilon^{24} - 8.6005\times10^{-11}\varepsilon^{26} + 3.34156\times10^{-9}\varepsilon^{28} + 1.63748\times10^{-9}\varepsilon^{30}.
\end{aligned} \tag{68}$$

The velocity is analytic in ε in the disk $|\varepsilon| < \varepsilon_0$. Therefore, (68) is valid for $\varepsilon < \varepsilon_0$, where ε_0 is of order $\frac{1}{b\chi}$, with χ being the maximal wave number of $T(x_1, x_2)$ and $B(x_1, x_2)$. In order to calculate $K(\varepsilon)$ for $\varepsilon \geqslant \varepsilon_0$, one can apply Padé approximation to the polynomial (68) which agrees up to $O(\varepsilon^{32})$. The Padé approximant of the order $(10, 20)$ was written down in [13],

$$K_{10,20}(\varepsilon) = \frac{P_{10}(\varepsilon)}{Q_{20}(\varepsilon)}, \tag{69}$$

where

$$\begin{aligned}
&P_{10}(\varepsilon) = 1 - 3.14215\varepsilon^2 + 6.59346\varepsilon^4 + 34.7591\varepsilon^6 + 13.3065\varepsilon^8 + 1.53446\varepsilon^{10}, \\
&Q_{20}(\varepsilon) = 1 - 2.88846\varepsilon^2 + 5.81781\varepsilon^4 + 36.3643\varepsilon^6 + 22.2659\varepsilon^8 + 5.65641\varepsilon^{10} \\
&+0.675967\varepsilon^{12} + 0.033858\varepsilon^{14} + 0.000131\varepsilon^{16} - 0.000010\varepsilon^{18} + 0.000001\varepsilon^{20}.
\end{aligned} \tag{70}$$

This approximant yields $K_{10,20}(\varepsilon) \sim \varepsilon^{-10}$, as $\varepsilon \to \infty$. More generally one can conjecture that permeability decays as $K(\varepsilon) \sim \varepsilon^{\nu}$, as $\varepsilon \to \infty$, with some unknown negative exponent (index) ν. When a function $K(\varepsilon)$ at asymptotically large variable behaves as

$$K(\varepsilon) \simeq B\varepsilon^{\nu}, \quad \text{as } \varepsilon \to \infty\ , \tag{71}$$

then the index can be represented by the limit

$$\nu = \lim_{\varepsilon\to\infty} \varepsilon\, \frac{d}{d\varepsilon}\, \log K(\varepsilon)\ . \tag{72}$$

as explained in the Introduction.

Preprints (www.preprints.org) | NOT PEER-REVIEWED | Posted: 6 September 2020 doi:10.20944/preprints202009.0141.v1

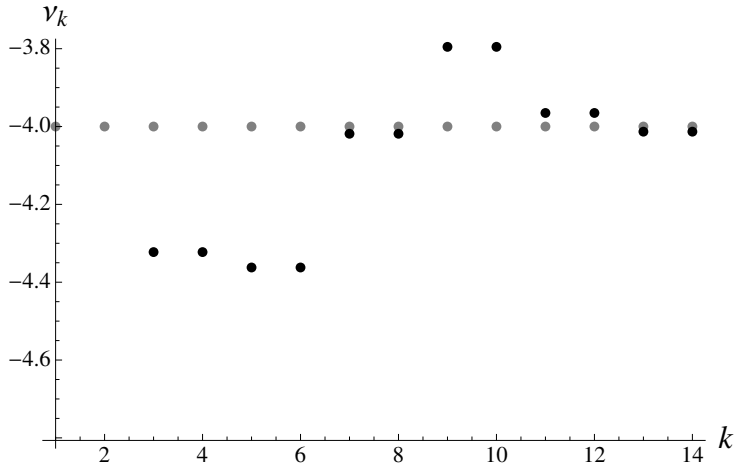

Figure 3: The index ν dependence on approximation number k is shown. The values calculated from (74), are shown with black circles, and compared with the most plausible value of -4 (shown with gray circles).

Assuming that the small-variable expansion for the function is given by the truncated sum $K_{tr}(\varepsilon)$, as in (68), we have the corresponding small-variable expression for the effective critical exponent

$$\varepsilon \, \frac{d}{d\varepsilon} \, \log K_{tr}(\varepsilon) \equiv N(\varepsilon). \tag{73}$$

By applying to the obtained series $N(\varepsilon)$ the method of diagonal Padé approximants, as has been discussed above, the sought approximate expression for the critical exponent is obtained,

$$\nu_k = \lim_{\varepsilon \to \infty} \varepsilon P_{k,k+1}(\varepsilon) \, , \tag{74}$$

which naturally depends on the approximation order k. Note that the value of the critical amplitude B does not enter the consideration at all. Application of the method to series of interest (68), is pretty much straightforward and suggests strongly the value of $\nu = -4$, as can be seen from Figure 3. The amplitude B, corresponding to $k = 14$, is equal to 44.5872. Assuming now that $\nu = -4$, we construct the sequence of Padé approximants $P_{n,n+4}$. There is a good convergence in approximation sequence for the amplitude B, to the value of 43.2 as shown in Fig. 4.

Preprints (www.preprints.org) | NOT PEER-REVIEWED | Posted: 6 September 2020 doi:10.20944/preprints202009.0141.v1

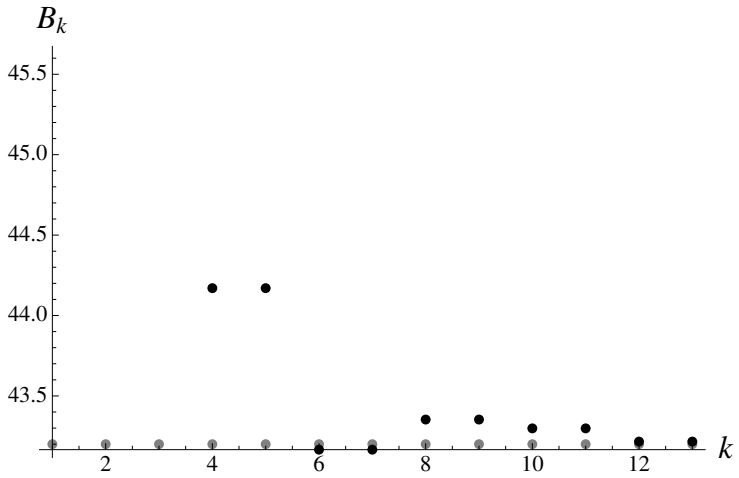

Figure 4: The amplitude B dependence on approximation number k is shown with black circles, with the convergence to the value of 43.2, shown with squares.

As the expression for permeability we suggest the Padé approximation of the order $(12, 16)$.

$$K_{12,16}(\varepsilon) = \frac{P_{12}(\varepsilon)}{Q_{16}(\varepsilon)}, \tag{75}$$

where

$$\begin{array}{l} P_{12}(\varepsilon) = 1 - 5.86404\varepsilon^2 - 3.84897\varepsilon^4 + 1.12295\varepsilon^6 + 0.867771\varepsilon^8 + \\ 0.151922\varepsilon^{10} + 0.00735283\varepsilon^{12}, \\ Q_{16}(\varepsilon) = 1 - 5.61035\varepsilon^2 - 5.31512\varepsilon^4 + 0.0206681\varepsilon^6 + 1.06989\varepsilon^8 + \\ +0.395962\varepsilon^{10} + 0.0645092\varepsilon^{12} + 0.0051812\varepsilon^{14} + 0.000170141\varepsilon^{16}. \end{array} \tag{76}$$

Comparison of the two Padé approximants is presented in Fig.5. Remarkably, the permeability can be expressed also through the factor approximant of relatively low order, which uses terms only up to the $14th$ order,

$$\begin{array}{l} \mathcal{F}^*_{14}(\varepsilon) = \\ (1 + (0.0925028 - 0.0501527i)\varepsilon^2)^{-0.957209-0.738327i} \times \\ (1 + (0.0925028 + 0.0501527i)\varepsilon^2)^{-0.957209+0.738327i} \times \\ (1 + (0.218267 - 0.101021i)\varepsilon^2)^{-0.042791+0.0798889i} \times \\ (1 + (0.218267 + 0.101021i)\varepsilon^2)^{-0.042791-0.0798889i}, \end{array} \tag{77}$$

Preprints (www.preprints.org) | NOT PEER-REVIEWED | Posted: 6 September 2020 doi:10.20944/preprints202009.0141.v1

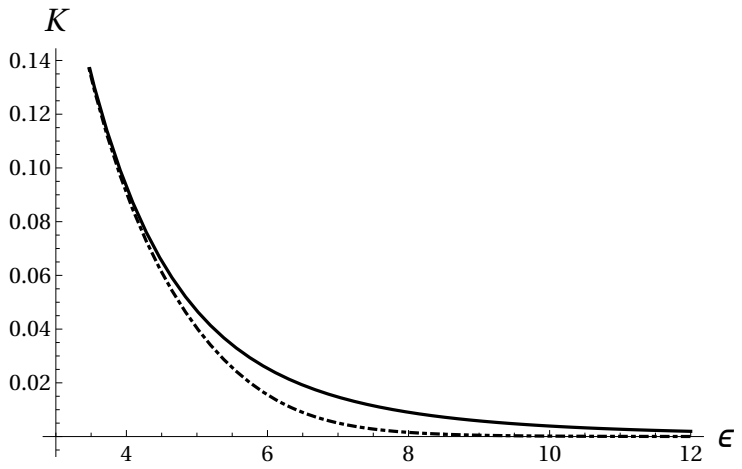

Figure 5: The two Padé approximants for permeability, $K_{10,20}$ (dot-dashed) and $K_{12,16}$ (solid) are compared.

which is very close to $K_{12,16}$, thus testifying for a high-quality of the original series. The factor approximant (77) is "smart", since it can predict three more coefficients, a_{16}, a_{18}, a_{20}, with average accuracy better than 1%. From (77) it also follows the value of amplitude $B = 43.3$, in agreement with calculations above. Note that the condition $\nu = -4$ was imposed in (77). Alternatively, we can use instead one more term from the expansion and find the index with practically unchanged value, $\nu \approx -4.02$.

3.2 Symmetric sinusoidal three-dimensional channel. Two-fluid model

Following [13] let us consider the channel restricted by the surfaces

$$z = \pm b\Big(1 + \frac{1}{2}\varepsilon\big(\cos(x+y) + \cos(x-y)\big)\Big), \tag{78}$$

with $b = 0.3$. The permeability is calculated up to $O(\varepsilon^{14})$

$$K_{14}(\varepsilon) = 1 - 0.465674\varepsilon^2 + 0.329218\varepsilon^4 - 0.261666\varepsilon^6 - 0.004467\varepsilon^8 - 0.0386987\varepsilon^{10} - 0.0177808\varepsilon^{12} - 0.0239319\varepsilon^{14}. \tag{79}$$

For $\varepsilon = \varepsilon_c = 1$, the surfaces (78) start touching, though the permeability remains finite at ε_c. The permeability series (79) is obtained with numerical

Preprints (www.preprints.org) | NOT PEER-REVIEWED | Posted: 6 September 2020 doi:10.20944/preprints202009.0141.v1

precision of 10^{-3} for values of ε up to 0.61. The "seepage" value of permeability at ε_c is considerable, $K_{14}(\varepsilon_c) = 0.517$, as is simply estimated from the series (79).

In the case being studied, application of the diagonal Padé approximants to (79), brings the following results: $P_{6,6}(\varepsilon_c) = 0.51277$, $P_{8,8}(\varepsilon_c) = 0.490636$. The full form of the higher order Padé approximants is given below,

$$\begin{array}{l} P_{6,6}(\varepsilon) = \frac{-0.272534\varepsilon^6+0.22825\varepsilon^4-0.657553\varepsilon^2+1}{-0.0363255\varepsilon^6-0.190321\varepsilon^4-0.191879\varepsilon^2+1}; \\ P_{8,8}(\varepsilon) = \frac{-0.266547\varepsilon^8-0.131478\varepsilon^6-0.363105\varepsilon^4+0.256413\varepsilon^2+1}{-0.0832011\varepsilon^8-0.273346\varepsilon^6-0.356065\varepsilon^4+0.722087\varepsilon^2+1}. \end{array} \tag{80}$$

It makes sense to establish bounds for the solution, and the upper and lower Padé bounds for $P_{6,6}(\varepsilon)$ are given as follows [1] :

$$\begin{array}{l} P_{6,4}(\varepsilon) = \frac{-0.25985\varepsilon^6+0.27733\varepsilon^4-0.664548\varepsilon^2+1}{-0.144498\varepsilon^4-0.198874\varepsilon^2+1}; \\ P_{6,8}(\varepsilon) = \frac{-0.354713\varepsilon^6+0.280003\varepsilon^4-0.721617\varepsilon^2+1}{-0.0476736\varepsilon^8-0.0872062\varepsilon^6-0.168401\varepsilon^4-0.255943\varepsilon^2+1}. \end{array} \tag{81}$$

We also constructed the two factor approximants. The first one, $\mathcal{F}^*_{12}(\varepsilon)$, is completely standard, while the second, $\mathcal{F}^*_{12,s}(\varepsilon)$, is "shifted" and conditioned in such a way that the (unknown) shift is supposed to give the sought value,

$$\begin{array}{l} \mathcal{F}^*_{12}(\varepsilon) = (1-0.867964\varepsilon^2)^{0.474676} \times \\ (1+(0.0821614+0.533783i)\varepsilon^2)^{1.35488+0.258822i} \times \\ (1+(0.0821614-0.533783i)\varepsilon^2)^{1.35488-0.258822i}; \\ \\ \mathcal{F}^*_{12,s}(\varepsilon) = 0.481814+0.518186\,(1-\varepsilon^2)^{0.766642} \times \\ (1-(0.074165+0.649541i)\varepsilon^2)^{1.46148+0.0652476i} \times \\ (1-(0.074165-0.649541i)\varepsilon^2)^{1.46148-0.0652476i}. \end{array} \tag{82}$$

Both approximants consume twelve terms from the expansion.

We are interested in the permeability at $\varepsilon = 1$. Thus, we have three estimates,

$$P_{6,6}(1) = 0.51277, \quad F^*_{12}(1) = 0.50195, \quad F^*_{12,s}(1) = 0.481814.$$

Their average K_{av} is equal to 0.498845, and corresponding margin of error can be estimated through the variance, which equals 0.0128272. Different formulas for the permeability are shown in in Fig.6.

Close to ε_c we simply find that

$$P_{6,6}(\varepsilon) \simeq 0.51277 + 2.30175(1-\varepsilon),$$

Preprints (www.preprints.org) | NOT PEER-REVIEWED | Posted: 6 September 2020 doi:10.20944/preprints202009.0141.v1

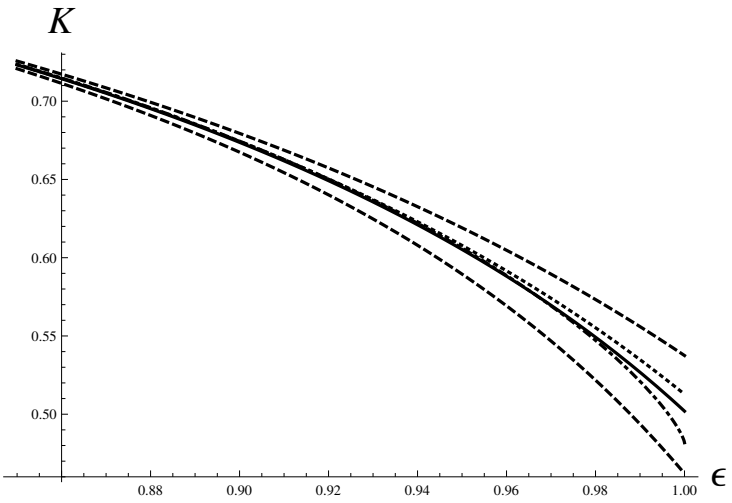

Figure 6: Bounds (81) for the permeability are shown with dashed lines. Comparison of the formulas in the vicinity of ε_c: Padé approximant $P_{6,6}$ is shown with with dotted line, factor approximant $\mathcal{F}^*_{12}$ from (82) is shown with solid line, and shifted factor approximant $\mathcal{F}^*_{12,s}$ from (82) is shown with dot-dashed line.

Preprints (www.preprints.org) | NOT PEER-REVIEWED | Posted: 6 September 2020 doi:10.20944/preprints202009.0141.v1

and the correction to constant is trivially linear. Similarly one can calculate

$$\mathcal{F}^*_{12,s}((\varepsilon) \simeq 0.481814 + 1.36825(1-\varepsilon)^{0.766642},$$

possibly indicating a non-trivial subcritical index of 0.767.

We would like to study in more detail the behavior of permeability in the vicinity of ε_c, assuming some deviations from linearity. Let us start with a more general initial approximation for the permeability which holds in the vicinity of $\varepsilon_c = 1$,

$$K_0(\varepsilon) \simeq A_0 + A_1(\varepsilon_c^2 - \varepsilon^2)^{\lambda_0}, \tag{83}$$

To find the unknowns we set from the start $A_0 = K_{av}$, and try to satisfy the expansion (79) in the second order. Then, $A_1 = 0.501155$, $\lambda_0 = 0.929201$. Expression (83) can be explained as a two-fluid model, since there are two components in the flow. One which is getting blocked by the obstacles to flow and another which can not be blocked.

We should recognize here that (83) with its parameters is only a crude approximation. In what follows let us attempt to correct the formula $K_0(\varepsilon)$, assuming instead of λ_0 some more general functional dependence $\Lambda^*(\varepsilon)$. As $\varepsilon \to \varepsilon_c$, $\Lambda^*(\varepsilon) \to \lambda_c$, the sought corrected value. The function $\Lambda^*(\varepsilon)$ will be designed in such a way, that it smoothly interpolates between the initial value λ_0 valid at small ε, and the sought value λ_c valid as $\varepsilon \to \varepsilon_c$. The corrected or "dressed" permeability $K^*(\varepsilon)$ is now given as follows:

$$K^*(\varepsilon) = A_0 + A_1(\varepsilon_c^2 - \varepsilon^2)^{\Lambda^*(\varepsilon)}, \tag{84}$$

and should be valid for all ε. From (84) one can express $\Lambda^*(\varepsilon)$, but only formally since $K^*(\varepsilon)$ is not known. But we can use its asymptotic form (79), express $\Lambda^*(\varepsilon)$ as a series for small ε, and apply some resummation procedure (e.g. Padé technique) in order to extend the series to the whole region of ε. Finally we calculate the limit of the approximants as $\varepsilon \to \varepsilon_c$ and find corrected value $\lambda_c = \Lambda^*(\varepsilon_c)$.

In what follows the $p(\varepsilon) = K_{14}(\varepsilon)$ stands for an asymptotic form of $K^*(\varepsilon)$ as $\varepsilon \to 0$. Corresponding asymptotic expression for Λ^*, just called $\Lambda(\varepsilon)$, can be made explicit from the following relation,

$$\Lambda(\varepsilon) \simeq \frac{\log\left(-\frac{(A_0 - p(\varepsilon))}{A_1}\right)}{\log(\varepsilon_c^2 - \varepsilon^2)}, \tag{85}$$

Preprints (www.preprints.org) | NOT PEER-REVIEWED | Posted: 6 September 2020 doi:10.20944/preprints202009.0141.v1

which can be explicitly presented as expansion in powers of ε around the value of λ_0,

$$\Lambda(\varepsilon) = \lambda_0 + \Lambda_1(\varepsilon). \tag{86}$$

It appears that one can construct now a sequence of diagonal Padé approximants

$$\Lambda_n(\varepsilon) = \lambda_0 + PadeApproximant[\Lambda_1[\varepsilon], n, n]), \tag{87}$$

with the sought limit $\Lambda^*(\varepsilon)$. Now we are able to estimate the critical index $\lambda_c = \Lambda^*(\varepsilon_c)$ and reconstruct the whole expression (84).

There is a good convergence within the approximations for the λ_c generated by the sequence of Padé approximants, corresponding to their order increasing:

$$\lambda_{c,1} = 0.929201, \quad \lambda_{c,2} = 0.402904, \quad \lambda_{c,4} = 0.631631,$$

$$\lambda_{c,6} = 0.630229, \quad \lambda_{c,8} = 0.702766, \quad \lambda_{c,10} = 0.698385 \quad \lambda_{c,12} = 0.702563.$$

Remarkably, in the highest orders (up to 18-th) the value of index remains practically the same. The final estimate for λ_c can be conjectured to be rational $\frac{2}{3}$.

The function $\Lambda^*(\varepsilon)$ needed to reconstruct the permeability, can be expressed as the Padé approximant. For instance, the approximant corresponding to $\lambda_{c,6}$ has the following form,

$$K_6^*(\varepsilon) = 0.498845 + 0.501155\left(1-\varepsilon^2\right)^{\frac{-4.15886\varepsilon^6+6.957\varepsilon^4-7.18244\varepsilon^2+0.929201}{-1.56421\varepsilon^6+2.06925\varepsilon^4-6.98732\varepsilon^2+1}}. \tag{88}$$

Formula (88), as well as the approximant (89), corresponding to $\lambda_{c,8}$,

$$K_8^*(\varepsilon) = 0.498845 + 0.501155\left(1-\varepsilon^2\right)^{\frac{0.134578\varepsilon^8-0.22113\varepsilon^6+0.650924\varepsilon^4-0.904689\varepsilon^2+0.929201}{-0.0295078\varepsilon^8-0.199491\varepsilon^6+0.298201\varepsilon^4-0.23125\varepsilon^2+1}}, \tag{89}$$

are confidently located within the Padé-bounds (81).

Formulas for the permeability including the subcritical regime, are shown in in Fig.7.

Thus, in the case of channel with wavy walls, the lubrication approximation works poorly, except when the surfaces are sufficiently close to a plane and for small value of ε. Different methodology, not involving lubrication approximation, is developed above. Closed-form expressions for arbitrary ε work rather well in both situations considered above, when walls can or cannot touch. In the former case, for the first time critical exponents and

Preprints (www.preprints.org) | NOT PEER-REVIEWED | Posted: 6 September 2020 doi:10.20944/preprints202009.0141.v1

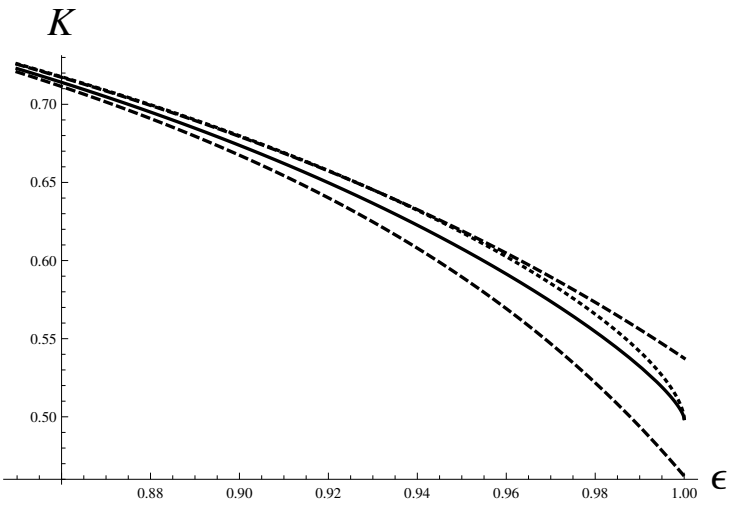

Figure 7: Bounds (81) for the permeability are shown with dashed lines. Comparison of the formulas in the vicinity of ε_c: $K_6^*(\varepsilon)$ is shown with dotted line, $K_8^*(\varepsilon)$ is shown with solid line.

amplitudes are calculated without invoking the lubrication approximation. In the latter case we discuss a crossover form the high-permeable to low-permeable state of the channel, characterized with the power low and corresponding exponent for large ε, also not invoking lubrication theory. Tiny viscous eddies dominate in this case, their onset over the whole length of the channel explains the quantitative breakdown of the lubrication approximation for the macroscopic quantity, such as permeability (59). The critical exponent though, is correctly estimated from the lubrication approximation (59), as the flow can still pass through the narrow channels between the eddies considered as cylinders. For the important case of a symmetric sinusoidal three-dimensional channel we also discussed possibility of a nontrivial sub-critical index and calculated its value.

4 Relaxation phenomena in time series

For the occurrence of a phenomenon, the original underlying symmetry must be broken. While studying the phenomenon it is important to distinguish between an explicit symmetry breaking when dynamical equations are not

Preprints (www.preprints.org) | NOT PEER-REVIEWED | Posted: 6 September 2020 doi:10.20944/preprints202009.0141.v1

invariant under the symmetry considered and spontaneous symmetry breaking, without presence of any asymmetric cause [29]. When successful, the approach based on broken global symmetries leads to understanding of the key phenomena of magnetism, superconductivity and superfluidity. On the other hand, when some global inherent symmetry can be recognized in physical quantities, we arrive to gloriously successful theory of critical phenomena and vital extensions of perturbation results in quantum field theories, jointly called renormalization group (RG). In a nutshell, below we suggest how to apply symmetry considerations to the crashes which occur in time series, with most notable example given by stock market crashes.

Assume that numerical data on the time series variable (e.g., price) s is given for some time t segment. There is a sequence of $N+1$ values $s(t_0), s(t_1) \ldots, s(t_N)$, for $N+1$ equidistant successive moments in time $t = t_j$, with $j = 0, 1, 2 \ldots, N$. In time series, one is interested in the extrapolated to future value of s. In financial mathematics, one is particularly interested in the predicted value of log return [35, 38],

$$R(t_N + \delta t) = \ln\left(\frac{s(t_N + \delta t)}{s(t_N)}\right). \tag{90}$$

One can see from the definition that we are really interested in the quantity $\mathbf{S} = \ln(s)$, to be called return. Let us place origin at the very beginning of the time interval, setting also $t_0 = 0$. Naturally, one is interested in the value of $\mathbf{S}(t_N + \delta t)$, allowing to find $R(t_N + \delta t)$ at a later time. Since the approach developed in [35, 28], is invariant with respect to the choice of time unit, we consider temporal points of the data set as integer, while consider the actual time variable as continuous.

Modern physics when applied to financial theory is concerned with ergodicity violations [30, 31, 32, 33]. Ergodicity violations may be understood as a manifestation of a non-stationarity, or violation of time-invariance of random process. Metastable phases in condensed matter also defy ergodicity over long observation timescales. In special quantum systems of ultracold atoms spontaneous breaking of time-translation symmetry could lead to formation of crystalline structures in time [34]. Concept of a spontaneously broken time-translation invariance can be useful for time series in application to market dynamics as first suggested in [35]. According to [35], window of forecasting of time series describing market evolution emerges due to a spontaneous breaking/restoration of the continuous time-translation invari-

 doi:10.20944/preprints202009.0141.v1

ance, dictated by relative probabilities of the evolution patterns [36]. In turn, the probabilities are derived from the stability considerations.

Notion of probability introduced in [36] is not based on the same conventional statistical ensemble probability for a collection of people, but is closer to the time probability, concerned with a single person living through time, see Gell-Mann, Peters [32], Taleb [33]. Probabilistic trading patterns correspond to local breakdown of time-translation invariance. Their evolution leads to the time-translation symmetry complete (or partial) restoration. We need to estimate typical time, amplitude and direction for such restorative process. Thus we are not confined to a binary outcome as in [35], but attempt to estimate also the magnitude of the event.

A catastrophic downward acceleration regime in the time series is known as crash [39]. Time series representing market price dynamics in the vicinity of crisis (crash, melt-up), could be treated as a self-similar evolution, because of prevalence of the collective coherent behavior of many trading, interacting agents [36, 40], including humans and machine algorithms. The dominant collective slow mode corresponding to such behavior, develops according to some law of collective motion, which could be expressed as a time-invariant, self-similar evolution. Away from crisis there is a superposition of collective coherent mode (generalized trend) and of a stochastic incoherent behavior of the agents [36, 38]. We do not attempt here to write down a generic evolution equation of behind the time series pertaining to market dynamics. Instead. we consider, locally in time, some trial functions-approximants, in the form inspired by the solutions to some well-known evolution equations. The approximants are designed to respect or violate the self-similarity. Our goal here is not of forecasting/timing the crash, but studying the crash as particular phenomenon created by spontaneous, time-translation symmetry breaking/restoration.

Since the market dynamics is believed to be formed by a crowd (herd) behavior of many interacting agents, there are ongoing attempts to create empirical, binary-type prediction markets functioning on such principle, or mini Wall Streets [37]. Prediction markets often work pretty well, however there are many cases when they give wrong prediction or make any prediction at all. Such special set-ups are already very useful in reaching understanding that market crowds are correct only if they express a sufficient diversity of opinion. Otherwise, market crowd can have a collective breakdowns, i.e., is fallible as expected by Soros [39].

 doi:10.20944/preprints202009.0141.v1

4.0.1 Self-similarity and time translation invariance

According to Isaac Newton and Murray Gell-Mann, the laws of nature are somehow self-similar. The laws of Newtonian mechanics are invariant with respect to Galilean group, expressing Galileo's principle of relativity [42],. The group includes time-translation invariance. Or else, the laws of classical mechanics are self-similar. What should be the underlying symmetry for price dynamics? Recall, that normal times are characterized by an approximate constant return (or price growth rate). This is equivalent to the statement that the average price trajectory is exponential, reflecting the power of compounding interests. Indeed, let s_{t_0} be an underlying security (index) price at $t = t_0$. Let F_t^P be the fair value of the future requiring a risk associated expected return β. Then (see, e.g.,[33]), expected forward price $F_t^P = s_{t_0} \exp(\beta(t - t_0)$. For example, a share of a stock would be correctly priced with the expected return calculated as the return of a risk-free money market fund minus the payout of the asset, being a continuous dividend for a stock. Thus, rather simple and natural exponential estimates are constantly made for the stocks and alike. The formula forward price is self-similar, or time-translation invariant, as explained below.

However, prices often deviate strongly from such simple description, forming bubbles, or other presumed patterns of technical analysis. There are intervals of time in which asset prices strongly deviate from the fundamental value. One of the practical problems of defining such intervals is that the fundamental value is not directly observable. The causes of deviation could be option hedging, portfolio insurance strategies, leveraging and margin requirements, imitation and herding behavior [39, 43]. These mechanisms tend to increase and accelerate the deviation from fundamental value.

Recall also that meaningful technical analysis starts from from recasting data in the form of some polynomial representation of the given data to serve as the expansion [35]. The regression is constructed in standard fashion by minimizing mean-square deviation, with the effective result that the high-frequency component of the price is getting average out. Then one can consider self-similarity in averages [40]. Indeed, the standard polynomial regressions are invariant under time-translation, retaining their form after arbitrary selection of origin of time with simple redefinition of all parameters. We put forward the idea that it is onset of broken time-translation invariance that signifies birth of a bubble, or of some other temporal pattern preceding crash. End of pattern corresponds to the restoration of time-translation

Preprints (www.preprints.org) | NOT PEER-REVIEWED | Posted: 6 September 2020 doi:10.20944/preprints202009.0141.v1

invariance, partially or fully. Our task is to express this idea in quantitative terms by making explicit transformation from the regression-based technical analysis to the valuation formula in the exponential form, bearing in mind taking into account strong deviations from the standard valuation formulae.

Assume that a time series dynamics is predominantly governed by its own internal laws. This is the same as to write down a self-similar evolution for the marker price s [44], meaning that for arbitrary shift τ one can see that

$$s(t+\tau, a) = s(t, s(\tau, a)), \tag{91}$$

with the initial condition $s(0, a) = a$ [45, 46]. The value of the self-similar function s in the moment $t+\tau$ with given initial condition, is the same as in the moment t, with the initial condition shifted to the value of s in the moment τ.

When t stands for true time, the property of self-similarity means the time-translation invariance. Formally understood equation (91) gives a background for the field-theoretical renormalization group, with addition of some perturbation expansion for the sought quantity, which should be resummed in accordance with self-similarity expressed in the form of ODE [45, 46, 47]. The time-translation invariance expressed by (91), means that the law for price evolution exists and remains unchanged with time, with proper transformation of the initial conditions [42]. The role of expansion when price dynamics is concerned, is accomplished by meaningful technical analysis, by recasting data in the form of some polynomial representation [35].

Consider first the simplest case of technical analysis. The linear function can be formally considered as the function of time and initial condition a, namely $s_1(t, a) = a + bt$, and $s_1(0, a) = a$. The linear function (regression) is self-similar, or time-translation invariant, as can be checked directly, by substitution to (91).

Through some standard procedure let us obtain the linear regression on the data around the origin $t_0 = 0$, so that

$$s_{0,1}(t) = a_1 + b_1 t.$$

Note that the position of origin is arbitrary, and it can be mode to arbitrary position given by real number r, so that

$$s_{r,1}(t) = A_1(r) + B_1(r)(t - r),$$

Preprints (www.preprints.org) | NOT PEER-REVIEWED | Posted: 6 September 2020 doi:10.20944/preprints202009.0141.v1

with new and different coefficients. It turns out that the coefficients are related as follows

$$A_1(r) = a_1 + b_1 r, \;\; B_1(r) = b_1,$$

so that

$$s_{r,1}(t) \equiv s_{0,1}(t).$$

By shifting origin we created an r-dependent form of the linear regression $s_{r,1}$, which can be used constructively. Thus instead of a single regression we have its r-replicas, equivalent to the original form of regression, and all replicas respect time-translation symmetry. In such sense one can speak about replica symmetry. Of course, we would like to avoid such redundancy in data parametrization.

The position of origin in time can be explicitly introduced into the regression formula and included into the coefficients, but actual results of calculations with any arbitrary chosen origin will remain the same. Such property can be expressed as some symmetry. However, intuitively, one would expect that the result of extrapolation with chosen predictors should be dependent on the point of origin r. Indeed, various patterns such as "heads and shoulders", "cup-with-handle"," hockey stick", etc., considered by technical analysts do depend on where the point of origin is placed. In physics, the point of origin (Big Bang) plays a fundamental role. We should find the way to break the replica symmetry.

As discussed above it is exponential shapes that are natural in pricing. Exponential function

$$E(t, a) = a \exp(\beta t),$$

with initial condition a and arbitrary β, satisfy functional self-similarity as well. It can be replicated as

$$\begin{aligned} E_r(t) &= \alpha(r) \exp(\beta(t - r)), \\ \alpha(r) &= a \exp(\beta r). \end{aligned} \tag{92}$$

Having β dependent on r is going to *violate* the time-translation and replica symmetry. Instead of a global time-translation invariance, we have a set of r local "laws" near each point of origin. But having r in the formula (92) fixed by imposing some additional condition, or being integrated out, should *restore* the global time-translation invariance completely as long as the exponential function is considered. Moreover, stability of the exponential function is measured by the exponential function with same symmetry (see

 doi:10.20944/preprints202009.0141.v1

formula (94)). Not only exponential function is time-translation invariant, but the expected return β has the same property. For exponential functions the expected (predicted) value of return per unit time, exactly equals β. Note, that shifted exponential function $E_s(t,a) = c + (a-c)\exp(bt)$, with initial condition a and arbitrary b, c, is invariant under time-translation as well.

Another interesting symmetry is shape invariance [48], meaning

$$F^P_{t+\tau} = \mathsf{m} F^P_t,$$

and an exponential function is shape invariant with $\mathsf{m} = \exp(\beta\tau)$, leaving expected return unchanged. Mind that our task is to calculate β from the time series. In principle, one can think about breaking/restoration of shape invariance, as a guide for construction of the concrete scheme for calculations.

For critical phenomena an underlying symmetry of formula for observable, is scaling

$$\phi_{\lambda t} = \Lambda \phi_t,$$

where $\Lambda = \phi_\lambda$. The class of power laws, $\phi_t = t^\alpha$, with critical index α, is scaling-invariant. The central task is to calculate c. The statistical renormalization group formulated by Wilson, see. e.g. [49], explains well the critical index in equilibrium statistical systems. When information on the critical index is encoded in some perturbation expansion, one can use resummation ideas to extract the index, even for short expansions and for non-equilibrium systems [50, 2, 9]. Some of the methods were discussed in the Introduction.

Working with power-law function will not leave the return unchanged. Yet, one can envisage the scheme with broken scaling invariance, as alternative to the former schemes. The log-periodic solutions extend the simple scaling [56], and are extensively employed in the form of a sophisticated seven-parametric fit to long historical data set [43], as well as of its extensions [57]. The fit is tuned for prediction of the crossover point to a crash, understood as catastrophic downward acceleration regime [39]. But one can not exclude the possibility of the solutions with different time of symmetries (scaling and time-invariance, for instance) competing to win over, or to coexist, all measured in terms of their stability characteristics.

Our primary concern is crash per se, not the regime preceding it. We start analyzing crash with the polynomial approximation that respects time-translation symmetry, then have the symmetry broken, and then restored (completely, or partially), by means of some optimization. Such sequence

 doi:10.20944/preprints202009.0141.v1

ends with a non-trivial outcome: β becomes renormalized $\beta(r)$, with r to be found from optimization procedure(s) defined below.

In the paper [35], the framework for technical analysis of time series was developed based on second-degree regression and asymptotically equivalent exponential approximants, with some rudimentary, implicit breaking of the symmetry. We intend to go to higher-degree regressions and and develop some consistent technique for explicit symmetry breaking with its subsequent restoration. According to textbooks, fourth order should be considered as "high". Taleb, see footnote on p.53 in [33], also considers models with five parameters as more than sufficient.

4.1 Optimization, approximants, multipliers

Higher-order regressions allow for replica symmetry. For instance, the quadratic regression $s_{0,2}(t) = a_2 + b_2 t + c_2 t^2$, can be replicated as follows:

$$s_{r,2}(t) = A_2(r) + B_2(r)(t-r) + C_2(r)(t-r)^2,$$

with

$$A_2(r) = a_2 + b_2 r + c_2 r^2,\ B_2(r) = b_2 + 2c_2 r,\ C_2(r) = c_2.$$

With such transformed parameters we find that $s_{r,2}(t) \equiv s_{0,2}(t)$. In fact, one can still formulate self-similarity analogous to (91), but in vector form with increased number of parameters/initial conditions in place of a [47]. But if only the linear part of quadratic regression, or trend, is taken into account, we return to the conventional functional self-similarity $\equiv$ time-translation invariance, discussed above extensively.

Such effective linear/trend approach to higher-order regressions allows to apply the same idea in all orders and observe how the exponential structures change with increasing regression order.

To take into account the dependence on origin, the replica symmetry has to be broken. Breaking of the symmetry means the dependence on origin of actual extrapolations with non-polynomial predictors. As the primary predictors we suggest the simplest exponential approximants considered as the function of origin r and time,

$$E_1^*(t,r) = A(r)\exp\left(\frac{B(r)}{A(r)}\,(t-r)\right), \tag{93}$$

independent on the order of polynomial regression. The approximants (93) are constructed by requiring an asymptotic equivalence with linear part of

 doi:10.20944/preprints202009.0141.v1

chosen polynomial regression. If the extrapolations $E_1^*(t_N + \delta t, r)$ are made by each of the approximants, they appear to be different for various r, meaning breaking of the replica symmetry and of the time-translation symmetry. Passage from polynomials to exponential functions leads to emergence of the continuous spectrum of relaxation (growth) times.

To compare the approximants quality, on can look at their stability. Stability of the approximants is characterized by the so-called multipliers defined as the variation derivative of the function with respect to some initial approximation function [36]. Following [58], one can take the linear regression as zero approximation, and find the multiplier

$$M_1^*(t, r) = \exp\left(\frac{B(r)}{A(r)}(t - r)\right). \tag{94}$$

The simple structure of multipliers (94) allows to avoid appearance of spurious zeroes which often complicate analysis with more complex approximants/multipliers.

Because of multiplicity of solutions, embodied in their dependence of origin, it is both natural and expedient to introduce probability for each solution. As explained in [36], one can introduce

$$Probability \propto |M_1^*(t, r)|^{-1},$$

with proper normalization, as shown below in formula (96). Probability appears to be of a pure dynamic origin and is expressed only from the time series itself. When the approximants and multipliers of the first order are applied to the starting terms of the quadratic, third or fourth order regression, we are confined to *effective first-order models*, with velocity parameter from [35] dependent also on higher order coefficients and origin.

To make extrapolation with approximants (93) one has still to know the origin. In other words, the time-translation symmetry has to be restored completely or partially, so that a specific predictor with specifically selected origin but, otherwise as close as possible to time-translation invariant form, is devised. Fixing unique origin also selects unique relaxation (growth) time during which the price is supposed to find a time-translation invariant state. Exponential functions are chosen above because they are invariant under time translation. Any shift in origins is absorbed by the pre-exponential amplitude and does not influence the return R. Similar in spirit view that broken symmetries have to be restored in a correct theory was expressed in [59].

Preprints (www.preprints.org) | NOT PEER-REVIEWED | Posted: 6 September 2020 doi:10.20944/preprints202009.0141.v1

In the approach predominantly adopted in this section, we keep the form and order of approximants the same in all orders, but let the series/regressions evolve into higher orders. Independent on the order of regression, we construct the same approximant, based only on the first order terms, only with parameters changing with increasing order of regression. In the framework of the effective first order theories, we employ exponential approximants.

Consider the value of origin as an optimization parameter [28]. To find it and to restore the time-translation symmetry, we have to impose an additional condition directly on the exponential predictors with known last closing price,

$$E_1^*(t_N, r) = s_N \,. \tag{95}$$

One has to solve the latter equation to find the particular origin(s) $r = r^*$. In this case we consider a discrete spectrum of origins, consisting of several isolated values. To avoid double-counting when the last closing price enters both regression and optimization, one can determine the regression parameters in the segment limited from above by t_{N-1}, s_{N-1}. Or, alternatively, one can consider the two ways to define regression parameters and choose the one which leads to more stable solutions. Unless otherwise stated, we consider that such comparison was performed and the most stable way was selected.

The extrapolation for the price is simply $s(t_N+\delta t) = E_1^*(t_N+\delta t, r^*)$. The condition imposed by the equation (95) is natural, because then, a first-order approximation to the formula (90), $R \approx \frac{s(t_N+\delta t)-s(t_N)}{s(t_N)}$, is recovered (see, e.g., [38]), as one would expect intuitively.

The procedure embodied in (95), leads to a radical reduction of the set of r-predictors to just a few. Set of predictors and corresponding to each multiplier, define the probabilistic, poor man's order book. Instead of an unknown to us true numbers of buy and sell orders, we calculate a priori probabilities for the price going up or down and corresponding levels. Target price is estimated through weighted averaging developed in [36, 58], in its concrete form (96) given below.

For sake of uniqueness one can simply choose the most stable result among such conditioned predictors. One can also consider extrapolation with weighted average of all such selected solutions. With $1 \leq M \leq 6$ solutions, their weighted average $\overline{E}_1$ for the time $t_N + \delta t$ is given as follows,

$$\overline{E}_1(t_N + \delta t) = \frac{\sum_{k=1}^{M} E_1^*(t_N + \delta t, r_k^*) \, |M_1^*(t_N + \delta t, r_k^*)|^{-1}}{\sum_{k=1}^{M} |M_1^*(t_N + \delta t, r_k^*)|^{-1}}. \tag{96}$$

 doi:10.20944/preprints202009.0141.v1

Within the discrete spectrum we can find solutions with varying degree of adherence to the original data. They can follow data rather closely or be loosely defined by the parameters of regression. The former could be called "normal" solutions, and tend to be less stable, with multipliers ~ 1, but the latter are "anomalous" solutions, since they cut through the data, and typically are the most stable with small multipliers. Anomalous solutions are crashes (meltdowns), and melt-ups. Typical situation with the solutions in the discrete spectrum is presented in Fig.10. The novel feature introduced through (96), is that averaging is performed over all approximants of the same order, compatible with constraints expressed by (95).

One can also integrate out the dependence on origin r, considered as continuous variable, by applying an averaging technique of weighted fixed points suggested in [36]. The dependence on origin enters the integration limit through parameter T. Integration can be performed numerically for the simplest exponential predictors according to the formula

$$I(t,T) = \frac{\int_{t_0-T}^{t_N+T} E_1^*(X,t)\,|M_1^*(X,t)|^{-1}\,dX}{\int_{t_0-T}^{t_N+T} |M_1^*(X,t)|^{-1}\,dX}. \tag{97}$$

To optimize the integral we have to impose an additional condition on the weighted average/integral. It is natural to force it pass precisely through the last historical point.

$$I(t_N,T) = s(t_N), \tag{98}$$

and solve the latter to find the integration limit $T = T^*$. The sought extrapolation value for the price s is simply $I(t_N + \delta t, T^*)$.

As an additional condition to find origin, one can also consider the minimal difference requirement on the lowest order predictors, as first suggested in [40]. To this end one has to construct the second order super-exponential approximant

$$\begin{aligned} E_2^*(t,r) &= A(r)\exp\left(\frac{B(r)(t-r)\exp\left(\frac{C(r)(t-r)\tau(r)}{B(r)}\right)}{A(r)}\right), \\ \tau(r) &= 1 - \frac{B(r)^2}{2A(r)C(r)}, \end{aligned} \tag{99}$$

and minimize its difference with the simplest exponential approximant in the time of interest $t_N + \delta t$. Namely, one has to find all roots of the equation

$$\exp\left(\frac{C(r)\tau(r)(t_N+\delta t-r)}{B(r)}\right) = 1, \tag{100}$$

 doi:10.20944/preprints202009.0141.v1

with respect to real variable r. Corresponding multiplier

$$M_2^*(t,r) = \frac{1}{B(r)} \frac{\partial E_2^*(t,r)}{\partial t} ,$$

can be found as well.

The discrete spectrum optimization seems to be the most natural and transparent. Our goal is to find the approximants and probabilistic distributions in the last available historical point of time series. Crashes are attributed to the stable solutions with large negative r, meaning that origin of time has to be moved to the deep past to explain crash in near future. Preliminary results of [28], suggest that in overwhelming majority of cases, crash is preceded by similar, asymmetric probability pattern(s), of the type shown in figures below [1]. There are also additional solutions with multipliers of the order of unity, coming form with the region of moderate r, and it is often possible to find some rather stable upward solution for large positive r. One can think that for such stable time series as describing population dynamics, the region of moderate r gives relevant solutions, while for time series describing price dynamics all types of solutions exist simultaneously.

Within our approach to constructing approximants one can also try to exploit the second order terms in regression. Instead of exponential approximants one should try some other, higher order approximants, but with time-translation invariance property. Such approximants are presented below. They are considered *ad hoc*, because they can be written in closed from only in special, low-order situations. It is not feasible to extend them systematically into arbitrary high order, in contrast with approximants mentioned in the context of first approach. On the contrary, all approximants mentioned for the first approach, violate the time-translation invariance, and can not be used purpose of symmetry restoration. Hence, our interest in special forms with desired symmetry. But all three approaches could be applied simultaneously and complementary, since the price evolution can take various unexpected forms. Sometimes, it is even not possible to find stable solutions with third approach, but is possible with corrected approximants.

Recall that exponential function can be obtained as the solution to simple linear first order ODE. In search of second order approximants with time-translation invariance, we turned to some explicit formulas, emerging in the

[1] As noted in [41], Kahneman and Tversky explained that people tend to judge current events by their similarity to memories of representative events.

Preprints (www.preprints.org) | NOT PEER-REVIEWED | Posted: 6 September 2020 doi:10.20944/preprints202009.0141.v1

course of solving some first order ODE with added nonlinear term with arbitrary positive power, which generalizes ODE for simple exponential growth. It is known as Bertalanffy-Richards(BR) growth model [60, 61]. Among its solutions in the case of second-order nonlinear term, there is a celebrated logistic function [60], $L(t) = \frac{1}{q_2 + \frac{(1-q_1 q_2)\exp(-q_0 t)}{q_1}}$, where q_1 is the initial condition. The logistic function is widely used to describe population growth phenomena and is also known to be the solution to logistic equation of growth. The logistic function written in the form $L(t, q_1)$, dependent on the initial condition $L(0, q_1) = q_1$, with arbitrary q_0, q_2, is time-translation invariant. One can also introduce the second-order logistic approximant which generalizes logistic function [28]. In addition to describing situations with saturation at infinity, the logistic approximant include also the case of so-called finite-time singularity, which makes it redundant, since such solutions were excluded from the price dynamics [35].

Another solution to the Bertalanffy-Richards model in the case when the nonlinear term has power only slightly differing from unity, is known as Gompertz function [60],

$$G(t) = g_0 \exp(g_1 \exp(g_2 t)), \tag{101}$$

used to describe growth (relaxation, decay) phenomena. But, as we demonstrate in the very end of Introduction, it is possible to explain $G(t)$ directly from the resummation technique leading to the formula (19), without resorting to BR. Relaxation time(growth) behaves exponentially with time. Gompertz function is *log*-time-translation invariant.

One can consider the second order Gompertz approximant. It simply generalizes the Gompertz function. Namely, one can find Gompertz approximant in the following form

$$\begin{aligned} &G(t, r) = g_0(r) \exp(g_1(r) \exp(g_2(r)(t - r))), \\ &g_0(r) = A(r) e^{-g_1(r)}, \quad g_1(r) = \frac{B(r)}{A(r) g_2(r)}, \quad g_2(r) = \frac{2A(r)C(r) - B(r)^2}{A(r)B(r)}, \end{aligned} \tag{102}$$

with the multiplier

$$M_G(t, r) = \frac{g_0(r) g_1(r) g_2(r) e^{(g_1(r) e^{g_2(r)(t-r)} + g_2(r)(t-r))}}{B(r)}.$$

The Gompertz approximant, of course, is not limited to the situations with saturation at infinity, as it can describe also very fast decay (growth) at infinity.

Preprints (www.preprints.org) | NOT PEER-REVIEWED | Posted: 6 September 2020 doi:10.20944/preprints202009.0141.v1

With r to be found from some optimization procedure, the return R generated by Gompertz approximant, is time-translation invariant, and has a compact form

$$R(\delta t) = g_1(r)\exp(g_2(r)(t_N - r))(\exp(g_2(r)\delta t) - 1).$$

For small δt it becomes particularly transparent:

$$R(\delta t) \approx g_1(r)g_2(r)\exp(g_2(r)(t_N - r)) \times \delta t \equiv \frac{\delta t}{\tau(T_N, r)},$$

with the pre-factor giving the return per unit time. The inverse return per unit time has the physical meaning of the effective time for growth (relaxation)

$$\beta(t,r)^{-1} \equiv \tau(t,r) = (g_1(r)g_2(r))^{-1}\exp\left(g_2(r)(r-t)\right),$$

considered at the moment $t = T_N$. Here, we employed the the effective relaxation (growth) time (see Introduction), $\tau(t) = \left(\frac{d}{dt}\ \ln G(t)\ \right)^{-1}$, and replicated it. We can find the return for Gompertz approximant solely determined by relaxation

$$\mathbf{S}(t,r) = \frac{1}{\tau(t,r)},$$

and express the log return in a compact form

$$R(\delta t) = \mathbf{S}(t_N + \delta t, r) - \mathbf{S}(t_N, r).$$

Thus, the return for Gompertz approximant is purely dynamic quantity. If relaxation time is found from the data to be very large as it should be close to equilibrium conditions [62], we have no potential for returns, i.e., near-equilibrium yields dull, everyday mundane events that are repetitive and lend themselves to statistical generalizations [39]. If relaxation time is anticipated to be very short, we have potentially huge returns, and conclude that far-from-equilibrium conditions give rise to unique, historic events [39].

Gompertz approximant can go at infinity faster or slower than exponential, and in some important examples such difference amounting to a few percents, can be detected. The function $g_0(r)$, could be called a gauge function for the price, expressing arbitrariness of choice of the price unit, as it does not enter the return. The time-translation invariance of return and gauge invariance for the price are considered very desirable in price model

 doi:10.20944/preprints202009.0141.v1

formulation [35], both properties are pertinent to exponential and Gompertz approximations for the price temporal dynamics.

We are interested in market prices on a daily level, and consider only significant market price drops/crashes with magnitude more than 5.5%. Such magnitude is selected to be comparable to the typical yearly return of Dow Jones Industrial Average index. Typically, a 2% daily move is considered as big, but not at the times of various turmoils. It is widely accepted in practical finance that asset price moves in response to unexpected fundamental information. The information can be identified as well as the tone, positive versus negative. It is found that news arrival is concentrated among days with large return movements, positive or negative [64]. Spontaneously emerging narratives, a simple story or easily expressed explanation of events, might be considered as largely exogenous shocks to the aggregate economy [41]. Simply put, one should analyze what people are talking about in search for the source of economic fluctuations. Moreover, just like in true epidemics governed by evolutionary biology, mutations in narratives spring up randomly, just as in organisms in evolutionary biology, and if contagious generate unpredictable changes in the economy [41]. As noted in [65], panic on the market can be due to external shocks or self-generated nervousness. It is argued [66], that cause and effect can be cleanly disentangled only in the case of exogenous shocks, as it is only needed to select some interesting set of shocks to which price is likely to respond. Effects of positive and negative oil price shocks on the stock price need not be symmetric. In macroeconomics it is even accepted that only positive changes in the price of oil have important effects. Periods dominated by oil price shocks are reasonably easy to identify, and they can be indeed considered as exogenous and, often, strong, although difficult to model. Oil price shocks are the leading alternative to monetary shocks, and may very well have similar effects [66].

4.2 Example

Consider as example a 7.72% drop in the value of Shanghai Composite index related to the first COVID-19 crash, which occur on February 3, 2020. With $N = 15$, as recommended in [35], the following data points available,

$$s_0 = 3085.2, s_1 = 3083.79, s_2 = 3083.41, s_3 = 3104.8, s_4 = 3066.89, s_5 = 3094.88,$$

$$s_6 = 3092.29, s_7 = 3115.57, s_8 = 3106.82, s_9 = 3090.04, s_{10} = 3074.08, s_{11} = 3075.5,$$

Preprints (www.preprints.org) | NOT PEER-REVIEWED | Posted: 6 September 2020 doi:10.20944/preprints202009.0141.v1

$$s_{12} = 3095.79,\ s_{13} = 3052.14,\ s_{14} = 3060.75,\ s_{15} = 2976.53.$$

And the value of $s_{16} = 2746.61$ is to be "predicted". From the whole set of daily data we employ only several values of the closing price. Such coarse-grained description of the time series may be justified if one is interested in the phenomenon not dependent on the fine details, such as crash. In the examples presented below, we keep the number of data points per quartic regression parameter in the range from 3 to 4. Lower order calculations can be found in [28]. Here we show only the quartic regression

$$s_{0,4}(t) = a_4 + b_4 t + c_4 t^2 + d_4 t^3 + f_4 t^4,$$

and based on it optimized approximants and multipliers. It can be replicated as follows:

$$s_{r,4}(t) = A_4(r) + B_4(r)(t-r) + C_4(r)(t-r)^2 + D_4(r)(t-r)^3 + F_4(r)(t-r)^4,$$

with

$$A_4(r) = a_4 + b_4 r + c_4 r^2 + d_4 r^3 + f_4 r^4,\ B_4(r) = b_4 + 2c_4 r + 3d_4 r^2 + 4f_4 r^3,$$

$$C_4(r) = c_4 + 3d_4 r + 6f_4 r^2, \quad D_4(r) = d_4 + 4f_4 r, \quad F_4(r) = f_4.$$

With such transformed parameters we have $s_{r,4}(t) \equiv s_{0,4}(t)$.

Within the data shown in Fig.8, one can discern competing trends. First, let us show the data compared to the regression. There are two obvious trends, "up" and "down" as can be seen in Fig.8. Our analysis will indeed

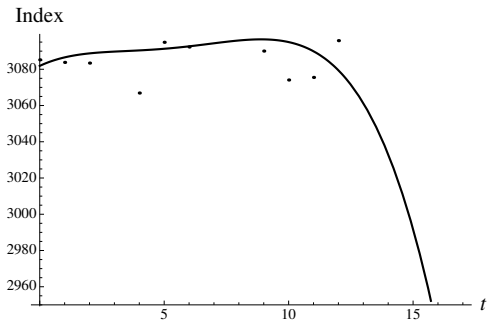

Figure 8: COVID-19, Shanghai Composite, February 3, 2020. Fourth-order regression against data points

Preprints (www.preprints.org) | NOT PEER-REVIEWED | Posted: 6 September 2020 doi:10.20944/preprints202009.0141.v1

find highly probable solutions of both types, with the downward trend developing into fast exponential decay. Let us analyze the typical approximant and multiplier dependencies on origin, for fixed time $t = t_N$. The inverse multiplier is shown as function of the origin r in Fig.9 as well as the first order approximant. There are two uneven humps in the probabilistic inverse

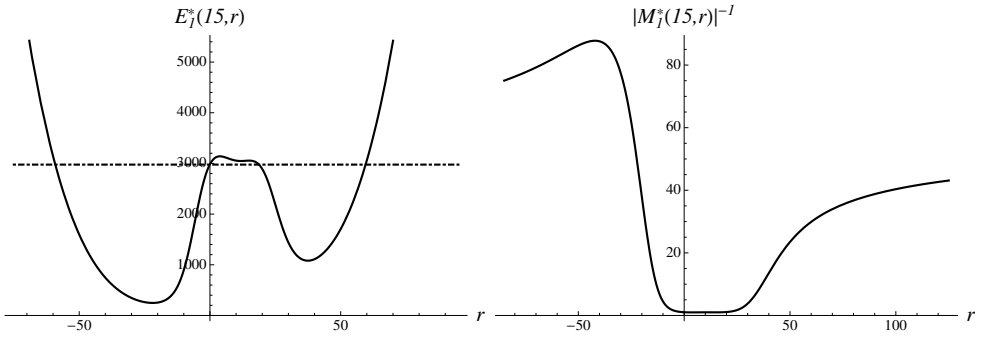

Figure 9: Shanghai Composite, February 3, 2020. Calculations with fourth-order regression. The inverse multiplier is shown as function of the origin r at $t = T_N$, $N = 15$. The first order approximant is shown at separate figure. Level s_{15} is shown as well, with dot-dashed line.

multiplier, suggesting that large negative and large positive r dominate, with more weight put on the negative region. Such dependence on r manifests the time-translation invariance violation, which should be lifted by finding appropriate origin. More details on the example can be found in [28]. Below we discuss only the fourth-order calculations.

The results of extrapolation by method expressed by equation (95) is given as

$$E_1^*(16) = 2804.32, \quad M_1^*(16) = 0.0113494,$$

with relative percentage error of 2.1%. There is also less stable "upward" solution

$$E_1^*(16) = 3211.95, \quad M_1^*(16) = 0.0363796,$$

in agreement with intuitive picture based on naive data analysis. There are also two additional solutions in between with multipliers close to 1. They do not effect averages much, but in real time the metastable solutions, just like metastable phases in condensed matter, may show up under special conditions. Metastable solutions when realized, violate principle of maximal sta-

Preprints (www.preprints.org) | NOT PEER-REVIEWED | Posted: 6 September 2020 doi:10.20944/preprints202009.0141.v1

bility over the observation timescale, complicating or even negating a unique forecast, based on weighted averages or the most stable solution.

Calculation of the discrete spectrum can be extended to different approximants. For instance, one can also construct the second order Gompertz approximant introduced above, and solve the following equation on origins,

$$G(t_N, r) = s(t_N)\,. \tag{103}$$

The most stable Gompertz approximant gives the most accurate estimate

$$G(16) = 2746.05, \quad M_G(16) = 0.001539,$$

with very small error of 0.02%. There are altogether five solutions to (103), in the discrete spectrum as shown in Fig.10. Thus, the Gompertz approximant

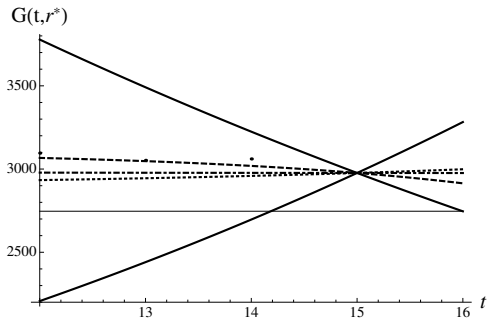

Figure 10: All Gompertz approximants corresponding to the discrete spectrum, i.e., solutions to (103) are shown. The most stable downward and less stable upward solutions are shown with solid lines. Three additional solutions are shown as well. The solution shown with dashed line is closest to the data. The "no-change", practically flat solution, is shown with dot-dashed line. Yet another solution, corresponding to moderate growth, is shown with dotted line. The level $s_{16} = 2746.61$ is shown with black line. Several historical data points are shown as well.

of second order with log-time-translation invariance, gives better results than symmetric exponential approximant E_1^*. Although Taleb's Black Swan did seem to materialize, the short-time stock market response was not different than in somewhat comparable instances of crashes brought up in [28], making it look like a Grey Swan. Indeed, it is plausible that a holiday season in

Preprints (www.preprints.org) | NOT PEER-REVIEWED | Posted: 6 September 2020 doi:10.20944/preprints202009.0141.v1

China, played the role here. It also helped our cause, effectively pinpointing the day for crash. One can think that all solutions, except the most extreme downward solution, where simply not considered.

4.3 Comments

Many more examples of various notable crashes can be found in [28]. They were selected to exemplify market reaction to shock including 9/11, Fukushima disaster, US entrance to the Great War, death of Chinese leader Deng Xiaoping, Friday the 13th, flash crash etc.,and to demonstrate similarity of early panics with coronavirus recession. Despite their different "geometry", different temporal patterns preceding crash, exhibit analogous in their main features probabilistic distributions, with significant difference only in the region of moderate r, but with analogous structure for large negative and positive origins. Crashes are attributed to the stable solutions with large negative r, meaning that origin of time has to be moved to the deep past to explain crash in near future. Preliminary results of [28], suggest that in overwhelming majority of cases, crash is preceded by similar, asymmetric probability pattern(s), of the type shown in figures of this section.

Exponential and Gompertz approximants are found to work rather well, despite(or due to?) their simplicity. Unlike all other approximants they give very clear graphic snapshot of the probabilistic space. Besides, their application is grounded in the exponential form of any future contract, with a transparent interpretation to the renormalized trend parameter $\beta(t, r)$, as expected return per unit time, equivalent to as inverse growth (relaxation) time.

Our theory explains or at least give a hint why making predictions about the future is so notoriously difficult. Instead of a unique, ironclad solution to the problem we advocate finding all solutions and interpret them as bounds as plainly illustrated in Fig.10. Bounds are given different strength, a priori determined by multipliers. Reality is not completely confined to reaching the most stable bound, but various metastable bounds can be realized as well, blurring the picture and complicating emergent time dynamics.

After applying some arguments concerned with broken/restored time-invariance, we come to the exponential solution with explicit finite time scale, which was only implicit in initial parametrization with polynomial regressions. Mind that in condensed matter physics and field theory there is a key Meissner-Higgs mechanism for generating mass or, equivalently, for

creating some typical space scale from original fields through broken symmetry technique (see, e.g.,[63]). Relatively recently the concept was confirmed, culminating in discovery of the Higgs boson. Our approach to market price evolution is by all means inspired by Meissner-Higgs effect. But, instead of a mass of mind-boggling elementary particle, we have a mundane, but highly sought after return per unit time.

References

[1] G.A.Baker, P. Graves-Moris, Padé approximants, Cambridge, UK: Cambridge University; 1996.

[2] S. Gluzman, V. Mityushev, W. Nawalaniec, Computational analysis of structured Media, Academic Press (Elsevier), 2017.

[3] I. Andrianov, J. Awrejcewicz, V. Danishevs'kyy, S. Ivankov, Asymptotic methods in the theory of plates with mixed boundary conditions, John Wiley & Sons, 2014.

[4] A. A. Gonchar, Rational approximation of analytic functions, Proceedings of the Steklov Institute of Mathematics, 272, Suppl.2: S44–S57, 2011.

[5] S. Gluzman, V.I. Yukalov, Effective summation and interpolation of series by self-similar approximants, Mathematics, 3, 510–526, 2015.

[6] S. Gluzman, V.I. Yukalov, D. Sornette, Self-similar factor approximants. Phys. Rev. E, 67, 026109, 2003.

[7] V. Yukalov, S. Gluzman, Self-similar exponential approximants, Phys. Rev. E. 58, 1359–1382, 1998.

[8] L.A. Gavrilov, N.S. Gavrilova, The reliability theory of aging and longevity, J.Theor.Biol.213, 527-453, 2001.

[9] P. Dryga' s, S. Gluzman V. Mityushev, W. Nawalaniec, Applied analysis of composite media, Woodhead Publishing (Elsevier), 2020.

[10] S. Torquato, Random heterogeneous materials: Microstructure and macroscopic properties, New York,Springer-Verlag: 2002.

 doi:10.20944/preprints202009.0141.v1

[11] P.M. Adler, Porous media. Geometry and transport, edition 2nd, New York, Butterworth-Heinemann; 1992.

[12] P.M. Adler, A.E. Malevich, V.V. Mityushev, Nonlinear correction to Darcy's law for channels with wavy walls, Acta Mech., 224, 2013. 1823–1848.

[13] A.E. Malevich, V.V. Mityushev, P.M. Adler, Stokes flow through a channel with wavy walls, Acta Mech.,182, 151–182, 2006.

[14] K.M. Golden, S.F. Ackley, V.I. Lytle, The percolation phase transition in sea ice,Science, 282, 2238–2241, 1998.

[15] K.M. Golden, Climate change and the mathematics of transport in sea ice, Science,56, 562–584, 2009.

[16] M. Murat, S. Marianer, D.J. Bergman, A transfer matrix study of conductivity and permeability exponents in continuum percolation, J. Phys. A., 1986; 19, L275–L279.

[17] M. J. Wolovick, J.C. Moore, Stopping the flood: could we use targeted geoengineering to mitigate sea level rise?, The Cryosphere, 12, 2955–2967, 2018.

[18] C. Pozrikidis, Creeping flow in two-dimensional channel, J. Fluid Mech.,180, 495–514, 1987.

[19] R. Wojnar, W. Bielski, Laminar flow past the bottom with obstacles – a suspension approximation. Bull. Pol. Acad. Sci., Tech. Sci. 63, 685–695, 2015.

[20] R. Wojnar, W. Bielski. Gravity driven flow past the bottom with small waviness. In: Drygas, P., Rogosin, S. (Eds.), Modern Problems in Applied Analysis. In: Trends in Mathematics. Birkhauser,181–202, 2018.

[21] W. Bielski, R. Wojnar. Stokes flow through a tube with wavy wall. In: Awrejcewicz, J. (Ed.), Dynamical Systems in Theoretical Perspective. DSTA 2017. In: Springer Proceedings in Mathematics & Statistics. Springer, Cham,379–390, 2018.

[22] M.Rasoulzadeh, M.Panfilov, Asymptotic solution to the viscous/inertial flow in wavy channels with permeable walls. Phys. Fluids 30, 106604. 2018.

[23] R. Czapla, V. Mityushev, W. Nawalaniec. Macroscopic conductivity of curvilinear channels. In: Jaworska, L. (Ed.), Int. Conf. Engineering, Education and Computer Science. Pedagogical University, Krakow, 2010.

[24] V. Mityushev, N. Rylko. Mathematical model of electrokinetic phenomena in two-dimensional channels. In: Jaworska, L. (Ed.), Int. Conf. Engineering, Education and Computer Science. Pedagogical University, Krakow, 5–20, 2010.

[25] P.M. Adler, J. Thovert, Fractures and Fracture Networks, edition 2nd, New York: Kluwer,1999.

[26] M. Scholle, Creeping Couette flow over an undulated plate, Arch. Appl. Mech.,73, 823–840, 2004.

[27] H. K. Moffatt, Viscous and resisitive eddies near a sharp corner, J.Fluid. Mech.,18, 1–18, 1964. See also H. K. Moffat: Corner flow : a classical problem with a new twist.: http://docslide.us/documents/hk-moffatt-corner-flow-a-classical-problem-with-a-new-twist.html

[28] S. Gluzman, Market crashes and time-translation invariance. Quantitative technical analysis, DOI: 10.13140/RG.2.2.22623.07842/1, June 2020.

[29] K. Brading, E. Castellani, N. Teh, Symmetry and symmetry breaking, The Stanford Encyclopedia of Philosophy (Winter 2017 Edition), Edward N. Zalta (ed.).

[30] O. Peters. Optimal leverage from non-ergodicity, Quant. Fin., 11, 593–1602, 2011.

[31] O. Peters, W. Klein, Ergodicity breaking in geometric Brownian motion, Phys. Rev. Lett., 110, 100603, 2013.

[32] O. Peters, M. Gell-Mann, Evaluating gambles using dynamics, Chaos. 26(2):023103, 2016.

 doi:10.20944/preprints202009.0141.v1

[33] N. N. Taleb, Statistical Consequences of Fat Tails (Technical Incerto Collection), 2020.

[34] K. Sacha, Modeling spontaneous breaking of time-translation symmetry, Phys. Rev. A 91, 033617, 2015.

[35] J. V. Andersen, S. Gluzman, D. Sornette, General framework for technical analysis of market prices, Europhys. J. B 14, 579–601, 2000.

[36] V.I. Yukalov, S. Gluzman, Weighted fixed points in self-similar analysis of time series, Int. J. Mod. Phys. B 13, 1463–1476, 1999.

[37] A. Mann, Market forecasts, Nature 538, 308–310, 2017.

[38] M. Fliess, C. Join, A mathematical proof of the existence of trends in financial time series, arXiv: 0901.1945v1 [q-fin.ST] 14 Jan 2009.

[39] G. Soros, Fallibility, reflexivity, and the human uncertainty principle, Journal of Economic Methodology, 20, 309-329, 2013.

[40] S. Gluzman, V. Yukalov, Renormalization group analysis of October market crashes, Mod. Phys. Lett. B 12, 75–84, 1998.

[41] R.J. Shiller, Narrative economics, American Economic Review 107, 967–1004, 2017.

[42] V. I. Arnold, Mathematical methods of classical mechanics, Springer-Verlag, 1989.

[43] Q. Zhang, Q. Zhang, D. Sornette, Early warning signals of financial crises with multi-scale quantile regressions of log-periodic power law singularities. PLoS ONE 11, e0165819, 2016.

[44] S. Gluzman, V. Yukalov, Booms and crashes of self-similar markets, Mod. Phys. Lett. B 12, 575–587, 1998.

[45] N. N. Bogoliubov, D. V. Shirkov, Quantum fields. Benjamin-Cummings Pub. Co., 1982.

[46] D.V. Shirkov, The renormalization group, the invariance principle, and functional self-similarity, Sov. Phys. Dokl. 27, 197–199, 1982.

[47] H. Kröger, Fractal geometry in quantum mechanics, field theory and spin systems, Phys. Rep. 323, 81–181, 2000.

[48] J. Bougie, A. Gangopadhyaya, J. Mallow, C. Rasinariu, Supersymmetric quantum mechanics and solvable models, Symmetry 4, 452–473; doi:10.3390/sym4030452, 2012.

[49] S. Ma, Theory of critical phenomena, Benjamin, London, 1976.

[50] S. Gluzman, V.I. Yukalov, Critical indices from self-similar root approximants, The European Physical Journal Plus 132: 535, 2017.

[51] S. Gluzman, V. I. Yukalov, Self-Similar Power Transforms in Extrapolation Problems, J. Math. Chem. 39, 47–56, 2006.

[52] V. I. Yukalov, S. Gluzman, Optimization of Self-Similar Factor Approximants, Molecular Physics, 107, 2237–2244, 2009.

[53] V. I. Yukalov, Statistical mechanics of strongly nonideal systems, Phys. Rev. A 42, 3324–3334, 1990.

[54] V. I. Yukalov, Method of self-similar approximations, J. Math. Phys., 32, 1235–1239, 1991.

[55] V.I. Yukalov, Stability conditions for method of self-similar approximations, J. Math. Phys., 33, 3994–4001, 1992.

[56] S. Gluzman, D. Sornette, Log-periodic route to fractal functions, art. no. 036142. Physical Review E, V6503 N3 PT2A:U418-U436, 2002.

[57] C. Lynch, B. Mestel, Logistic model for stock market bubbles and anti-bubbles, International Journal of Theoretical and Applied Finance, 20(6), article no. 1750038, 2017.

[58] V.I. Yukalov, S. Gluzman, Extrapolation of power series by self-similar factor and root approximants, Int. J. Mod. Phys. B 18, 3027–3046, 2004.

[59] T. Duguet, J. Sadoudi, Breaking and restoring symmetries within the nuclear energy density functional method, J.Phys.G: Nucl. Part. Phys. 37, 064009, 2010.

 doi:10.20944/preprints202009.0141.v1

[60] Y.C. Lei, S.Y. Zhang, Features and partial derivatives of Bertalanffy-Richards growth model in forestry, Nonlinear Analysis: Modelling and Control, 9, 65–73, 2004.

[61] F. J. Richards, A flexible growth function for empirical use, J. Exp Bot., 10, 290–301, 1959.

[62] S. Gluzman, D. Karpeev, Perturbative expansions and critical phenomena in random structured media, In Book "Modern Problems in Applied Analysis", Eds. P. Drygaś and S. Rogosin, 117–134, Birkhauser, 2017.

[63] H. Kleinert, Vortex origin of tricritical point in Ginzburg–Landau theory, Europhys. Lett., 74, 889–895, 2006.

[64] J. Boudoukh, R. Feldman, S. Kogan, M. Richardson, Which news moves stock prices? A textual analysis, NBER Working Paper No. 18725 January 2012,

[65] D. Harmon, M. Lagi, M. A. M. de Aguiar, D. D. Chinellato, D. Braha, I. R. Epstein, Y. Bar-Yam, Anticipating economic market crises using measures of collective panic, PLoS ONE 10(7): e0131871. doi:10.1371/journal.pone.0131871, 2015.

[66] B. S. Bernanke, M. Gertler, M. Watson, Systematic monetary policy and the effects of oil price shocks, Brookings Papers on Economic Activity, 1, 91–157, 1997.